A REVIEW OF AERONAUTICAL FATIGUE AND STRUCTURAL INTEGRITY IN ISRAEL (2023 –2025)

Compiled by:

Dr. Yuval Freed
Engineering & Development Center
Aviation Group
Israel Aerospace Industries
Ben-Gurion Airport, Israel
yfreed@iai.co.il

A REVIEW OF AERONAUTICAL FATIGUE AND STRUCTURAL INTEGRITY IN ISRAEL

JANUARY 2023 – DECEMBER 2024

SUMMARY

This review summarizes fatigue, structural-integrity and fracture-mechanics investigations that were performed in Israel during the period of January 2023 to December 2024. The review includes contributions from Israel Aerospace Industries Ltd. (IAI), Tel-Aviv University (TAU), Ben-Gurion University (BGU) and Ariel University (AU).

TABLE OF CONTENTS

A REVIEW OF AERONAUTICAL FATIGUE INVESTIGATIONS IN ISRAEL JANUARY 2017 – DECEMBER 2018

1. Introduction

The Israel National Review summarizes activities performed in the field of aeronautical fatigue, structural integrity, health monitoring and fracture mechanics in Israel during the period of January 2023 to December 2024. The previous National Review [1] covered activities up to the end of 2022. The following organizations contributed to this review:

- Israel Aerospace Industries Ltd. (IAI)
- Tel-Aviv University (TAU)
- Ben-Gurion University (BGU)
- Ariel University (AU)

The National Review was compiled by Dr. Yuval Freed (yfreed@iai.co.il).

2. Structural Integrity of Metallic Structures

2.1 Fatigue crack growth in monocrystals and polycrystals of Nickel (M. Perl, BGU)

Short fatigue cracks (SFCs) are a critical aspect of material fatigue studies, especially in polycrystalline metals. They present unique challenges due to their microscopic nature and their interaction with the complex grain structures of polycrystalline materials. This study [2] proposes that long fatigue cracks in monocrystals, which lack grain boundaries, can emulate the behavior of SFCs in polycrystals. Key characteristics of SFCs include:

1. The absence of a threshold stress intensity factor ΔK_I below which cracks do not propagate
2. Elevated fatigue crack growth rates (FCGR) at low ΔK_I
3. Erratic growth rates due to interactions with microstructural elements like grain boundaries

The experimental approach included fabricating compact tension specimens from pure nickel. Polycrystalline specimens were cut parallel to the cross-section of an extruded bar to minimize texture effects, while monocrystals were grown specifically for this study and oriented along two key crystallographic planes: (100) and (110). The specimens were electrochemically polished to ensure uniform surface conditions. The initial crack length was defined only after visible propagation on both surfaces of the specimens. Fatigue tests were conducted under cyclic loading at a frequency of 10 Hz and a load ratio R = 0.1. Crack growth was monitored using precision crack gauges and analyzed with optical, scanning electron microscopy (SEM), and atomic force microscopy (AFM).

The following key findings were reported:

- Threshold Stress Intensity Factors: Monocrystals exhibited a significantly lower threshold ΔK_I compared to polycrystals. This mirrors the behavior of SFCs, which propagate unimpeded by grain boundaries in their early growth phases. This reduction in threshold may be attributed to the intrinsic properties of monocrystals, including the absence of microstructural barriers

- Fatigue Crack Growth Rate (FCGR): The FCGR of monocrystals at low ΔK_I was higher than the corresponding rates in polycrystals. This behavior is consistent with SFCs in polycrystals, which grow faster in the absence of grain boundary obstacles during their initial phases. The Paris law region of the FCGR curve showed similarities between monocrystals and polycrystals, indicating comparable growth trends once cracks transition to steady-state propagation

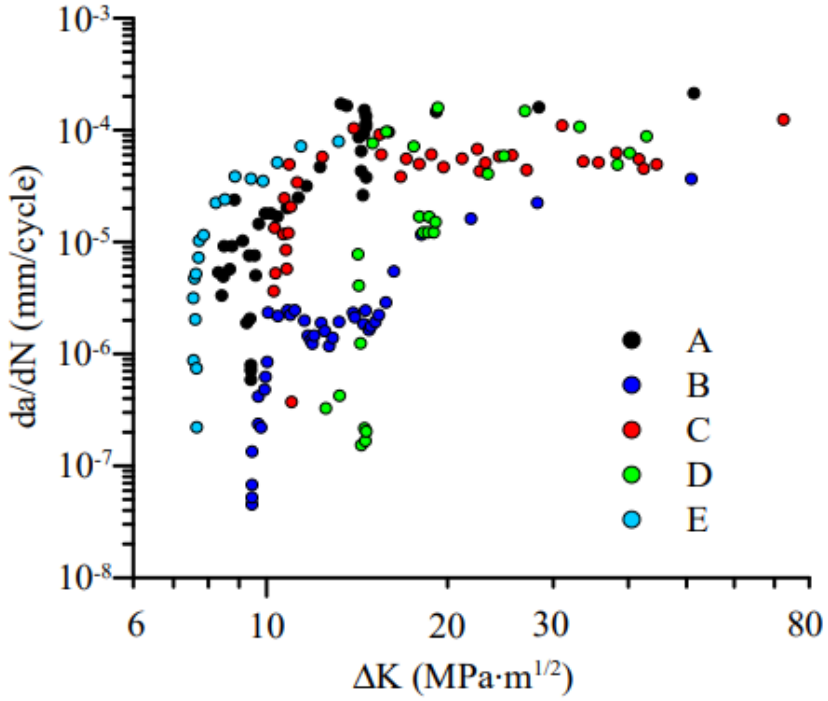

Figure 1. FCRG in five polycrystalline nickel specimens

- Erratic Growth Rates: In polycrystals, the randomness of the microstructure causes SFCs to encounter grain boundaries unpredictably, leading to variability in growth rates. Similarly, long cracks in monocrystals exhibited diverse FCGRs depending on crystallographic orientation, highlighting the influence of slip system activity on growth behavior

- Crystallographic Orientation Effect: The study examined two orientations in monocrystals, (110) and (100). For (110) orientation, cracks showed rough, deflected paths characterized by significant branching and crack closure effects. The crack roughness reduced the effective stress intensity factor, slowing the FCGR. This was evident in a relatively flat Paris law slope n = 1.1. For (100) orientation, cracks propagated smoothly with minimal deflection. The higher ΔK_I resulted in faster FCGR and a steep Paris law slope (n = 4.9)

- Slip System Activation: Slip activity was concentrated near crack tips, intensifying with increasing crack length. Slip planes above and below the crack plane were distinct, reducing strain hardening

- Metallurgical Observations: The study highlighted the role of crystallographic orientation in influencing crack propagation. For (110) orientation, double slip systems dominated, leading to deflected crack paths and rough fracture surfaces. For (100), Single slip systems predominated, resulting in smooth crack paths and higher FCGRs

- Fracture Surface Analysis: Fractographic observations revealed distinct features based on orientation. For (110), Brittle, ridge-like structures due to zig-zag crack propagation

were observed, whereas for (100) Ductile striations indicating planar crack growth were reported

The findings reported in this study validate that long fatigue cracks in monocrystals can serve as a model for SFC behavior in polycrystalline materials, capturing key characteristics like lower threshold ΔK_I higher FCGRs at low ΔK_I, and variability in growth rates. The study emphasizes the importance of crystallographic orientation in dictating crack path morphology and growth rates.

2.2 Increasing the load carrying capacity of hollow rotating disks by applying rotational autofrettage (M. Perl, BGU)

The study presented in this paper [3] explores the application of rotational autofrettage as a method to enhance the rotational load-carrying capacity of hollow rotating disks used in turbomachinery, such as gas turbines, flywheels, and brake rotors. It focuses on mitigating tensile stress-induced failures, particularly inner cracking, by introducing residual stresses. This innovative approach provides a significant improvement in operational safety and efficiency.

Rotating disks are integral components of various mechanical systems, transferring energy and performing essential design functions. They operate at extremely high rotational speeds, inducing significant tensile stresses, especially at the inner surface. This stress increases the susceptibility to cracking, which can lead to catastrophic failures. Rotational autofrettage, a prestressing technique that induces beneficial compressive hoop residual stresses, is proposed as a mitigation to such cracks.

Rotational autofrettage involves plastically deforming the inner portion of a rotating disk by subjecting it to a high-speed rotation beyond its yield-onset speed, followed by unloading. This process creates a compressive residual stress field at the inner surface while the outer regions bear tensile stresses. The method increases the maximum allowable rotational speed, thereby enhancing the disk's load-carrying capacity. Generally, The autofrettage process can be partial or full. In partial autofrettage, only the inner portion undergoes plastic deformation, while the outer remains elastic, whereas in full autofrettage the entire disk is plastically deformed during the process.

This study employs theoretical and numerical analyses using the von Mises yield criterion to evaluate the residual stress distribution and the load-bearing enhancement in autofrettaged disks. Disks with varying radii ratios r_2/r_1 ranging from 2 to 100 are analyzed, where r_1 and r_2 are the inner and outer radii, respectively. AISI 4340 steel was used for the simulations, and the maximum autofrettage speed to prevent reverse yielding and ensure the residual stresses remain below the material's yield strength during unloading was obtained.

The following key findings were reported:

- Stress distributions: During unloading, Smaller disks ($r_2/r_1 < 3$) undergo full autofrettage, achieving uniform plastic deformation. For larger disks ($r_2/r_1 > 3$) partial autofrettage was obtained, with plastic deformation limited to the inner region. Beyond the elastic-plastic interface radius, the material remains elastic. After unloading, residual hoop stress distributions show maximum compressive stresses at the inner surface, reducing toward the outer radius. Larger radii ratios achieve compressive stresses equal to the yield stress at the bore
- Load carrying capacity: gears with ($r_2/r_1 > 3.5$) achieve a maximum increase of more than 40% in rotational load-carrying capacity as compared to non-autofrettaged counterparts. For smaller disks, the increase varies between 24% and 37%

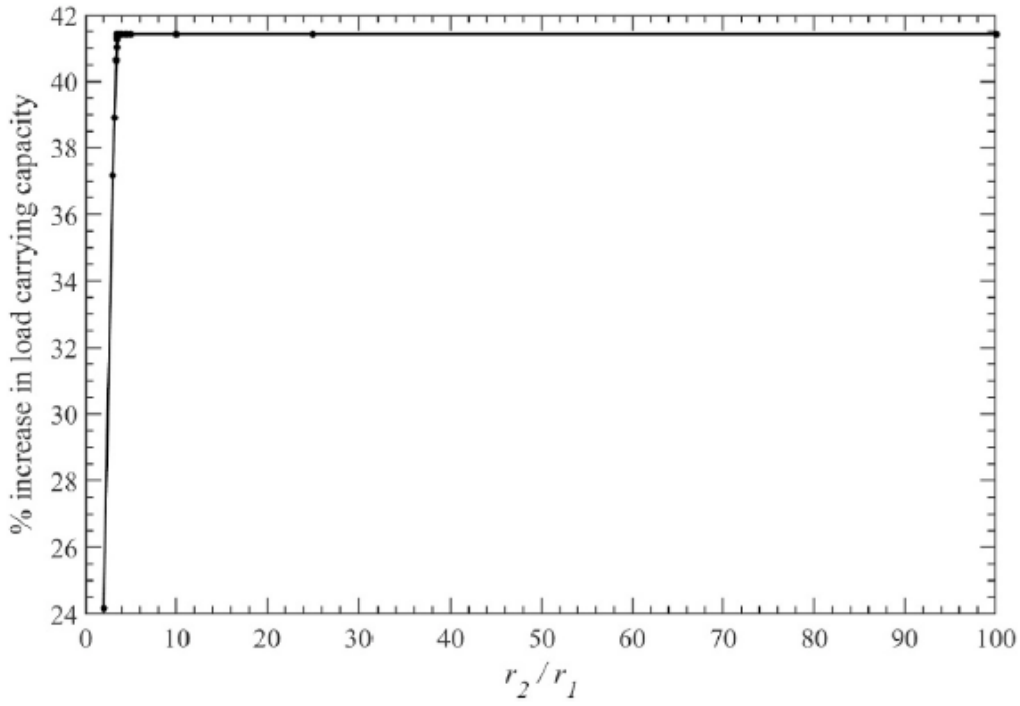

Figure 2. Relative increase in rotational load carrying capacity of rotationally autofrettaged disks as a function of the radii ratio

- Rotational autofrettage allows the use of materials with lower yield stress, which are typically tougher and more resistant to cracking. For instance, a disk made of AISI 4340 with a yield stress of 525 MPa (half of the original material used in this study) can achieve similar operational speeds after autofrettage while exhibiting better fatigue resistance and longer critical crack lengths

To conclude, this study establishes rotational autofrettage as a practical and effective method for increasing the load-carrying capacity of rotating disks. The findings reported highlight the potential of rotational autofrettage to revolutionize disk design, particularly in applications requiring high reliability and performance. Future work will explore the method's effects on crack suppression and its integration with advanced materials.

2.3 The Change in the SIF of an Internal Semi-Elliptical Surface Crack Due to the Presence of an Adjacent Nonaligned Corner Quarter-Circle Crack in a Semi-Infinite Plate Under Remote Bending (M. Perl, BGU)

In fracture mechanics, understanding Stress Intensity Factors (SIFs) is crucial for predicting crack propagation and assessing structural integrity. For components with multiple cracks, interaction effects significantly influence the SIFs. While the interaction between parallel cracks has been extensively studied, the impact of a corner quarter-circle crack on a semi-elliptical surface crack under bending has remained unexplored.

This study [4] evaluates the influence of geometrical parameters—horizontal separation (S), vertical gap (H), and relative crack sizes—on the SIFs of the surface crack. Using finite element analysis (FEA), the research models cracks in a semi-infinite steel plate under pure bending. The study employed 3D finite element modeling in ANSYS to calculate SIFs for various configurations. The semi-elliptical crack was modeled with varying ellipticity (b_1/a_1 = 0.1 to 1.0), while the corner crack had a fixed length. Simulations considered normalized horizontal and vertical separations to capture a wide range of interaction scenarios. To ensure accuracy, a sub-modeling technique was used, incorporating high-resolution meshing near the crack fronts. SIFs were computed along the semi-elliptical crack front at 9° intervals, capturing variations in stress distribution.

The following key findings were reported:

- Impact of crack interaction: The presence of the corner crack generally amplifies the SIFs along the semi-elliptical crack front, especially near the corner crack tip ($\varphi = 0°$). The amplification effect diminishes as the cracks are separated further horizontally or vertically, indicating that crack interaction weakens with distance
- Bending vs. Tension loading: Compared to uniaxial tension, bending results in lower SIFs due to the non-uniform stress distribution above the crack line. Despite lower SIF values, the interaction trends observed in bending largely parallel those in tension

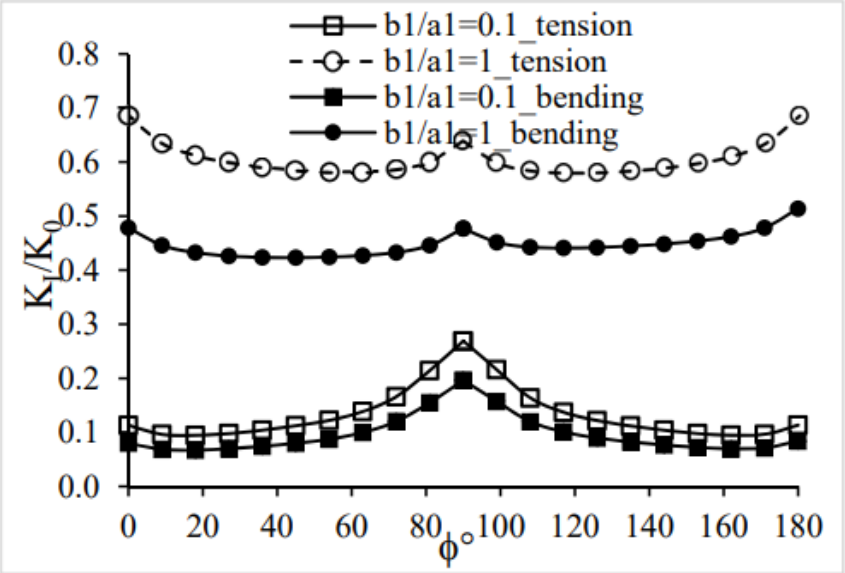

Figure 3. SIF distribution for a semi-elliptic surface crack when no corner crack is present both in bending and in tension

- Ellipticity and crack depth effects: Deeper semi-elliptical cracks (b_1/a_1 = 1) exhibit greater SIF amplification near the corner crack compared to shallow cracks (b_1/a_1 = 0.1). The cross-over effect, where the SIFs of the dual-crack system dip below those of the solitary crack system, was observed in certain configurations, particularly for shallow cracks and overlapping scenarios
- Separation distance and overlap: Horizontal separation plays a critical role; as cracks are aligned, the SIFs are significantly affected. Increased separation results in near-independent behavior of the cracks. Vertical separation also modulates interaction. Greater gaps lead to reduced amplification, with SIF distributions converging toward those of a single crack system.
- Size and alignment considerations: The relative size of the cracks influences the extent of interaction. Larger semi-elliptical cracks relative to the corner crack show more pronounced SIF amplifications

To conclude, this study highlights the importance of accounting for crack interactions in structural components under bending loads. The findings provide guidance on evaluating the combined effects of multiple cracks. Specifically, it underscores the need to consider crack geometry, alignment, and load conditions to avoid overly conservative or non-conservative assessments. The research also identifies shadowing effects where the presence of one crack reduces the SIFs of another, contrary to traditional expectations. Such phenomena emphasize the complexity of crack interactions and the necessity for detailed numerical analyses.

Future work may focus on extending these findings to other materials, load conditions, and complex geometries, further refining predictive models for crack interaction in engineering applications.

2.4 Modes I and II stress intensity factors for a slanted-edge-crack affected by an adjacent horizontal crack under remote tension (M. Perl, BGU)

Structural integrity assessments of components containing multiple cracks are essential in engineering disciplines such as pressure vessels and piping. Most prior studies have focused on aligned or parallel cracks, leaving the interaction of non-parallel cracks underexplored. This study [5] aims to quantify the Mode I (tensile opening) and Mode II (in-plane shear) SIFs for a slanted edge crack influenced by an adjacent horizontal crack.

The study uses a 2D finite element analysis (FEA) to model a semi-infinite steel plate with one edge slanted crack and one horizontal embedded crack. Key variables include the slanted angle (β) of the edge crack, the vertical (H) and horizontal (S) separation distances between cracks, and their respective lengths (a_1 and a_2). The material is assumed to have plane strain conditions, with properties typical of steel (e.g., Young's modulus of 200 GPa). ANSYS software is used for modeling, and results are normalized for consistency with established literature.

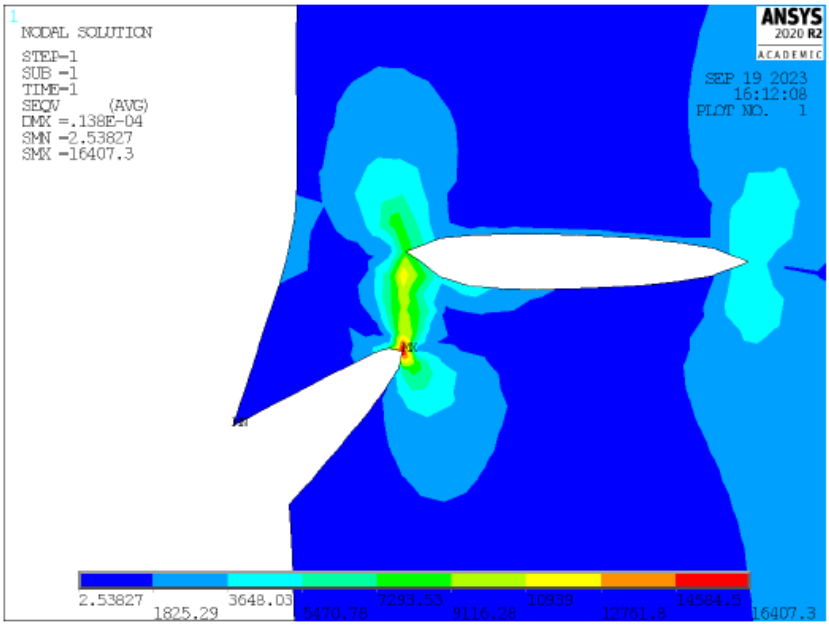

Figure 4. A typical contour plot of von-Mises stress field in the vicinity of the cracks

The following key findings were reported in this study:

- Amplification of Mode I SIFs: The embedded crack always amplifies the Mode I SIF at the tip of the slanted edge crack. This amplification increases with the slant angle β and decreases as the horizontal separation (S/a_2) grows. For overlapping cracks ($S/a_2 \leq 0$), the amplification is more pronounced
- Mixed Effects on Mode II SIFs: The presence of the embedded crack can either amplify or attenuate the Mode II SIF, depending on the relative crack positions and β. For non-

overlapping cracks ($S/a_2 > 0$), amplification predominates, while overlapping configurations ($S/a_2 \leq 0$) often exhibit attenuation

- Effect of Crack Size Ratio (a_2/a_1): When the edge crack is smaller ($a_2/a_1 < 1$), both Mode I and Mode II SIFs are significantly amplified. Conversely, when the edge crack is larger ($a_2/a_1 > 1$), crack shielding effects can attenuate the SIFs, particularly for Mode II
- Behavior with Increasing Separation: As the horizontal separation S/a_2 increases, the influence of the embedded crack diminishes, and the SIFs approach those of a solitary edge crack
- Crack Shielding: For certain configurations, especially when $a_2/a_1 > 1$, the embedded crack shields the edge crack, reducing its SIFs compared to the solitary case. This effect is most pronounced for small slant angles and overlapping cracks

This research underscores the need for accurate modeling of non-parallel crack interactions in structural assessments. The results can improve the safety and reliability of engineering components subjected to fatigue and stress corrosion cracking. By addressing the complex behavior of non-parallel cracks, the study contributes to the broader understanding of fracture mechanics and its practical applications in critical infrastructure.

2.5 An investigation into semi-stabilized unsymmetrical thin-walled structure (S. Katzeff, IAI)

In semi-monocoque aircraft primary structure, thin-walled metallic sections are fastened or bonded to external skin to carry load in both hoop and longitudinal directions. Although symmetrical sections are preferred, practical design constraints sometimes necessitate unsymmetrical sections. It is generally assumed that these geometrically unsymmetrical sections are structurally equivalent. This assumption stems from the concept that the member is considered stabilized; meaning that it is prevented from deflecting in the transverse direction through its attachment to the skin. Such simplification allows engineers to analyze the section as if it were symmetrical, using standard bending formulas to calculate stress, primarily along the global horizontal axis.

The 'abstract' product of inertia Ixy is typically ignored, allowing the structure to be considered fully stabilized. However, this assumption is non-conservative. Even a stabilized unsymmetrical section requires an additional stabilizing transverse moment at its attachments to stabilizing members, such as aircraft skin. The non-conservatism becomes more pronounced in structures stabilized at only one outstanding flange—a condition termed semi-stabilized. In such configurations, fewer fasteners or reduced bonding are needed to apply the stabilizing transverse moment, potentially compromising structural integrity.

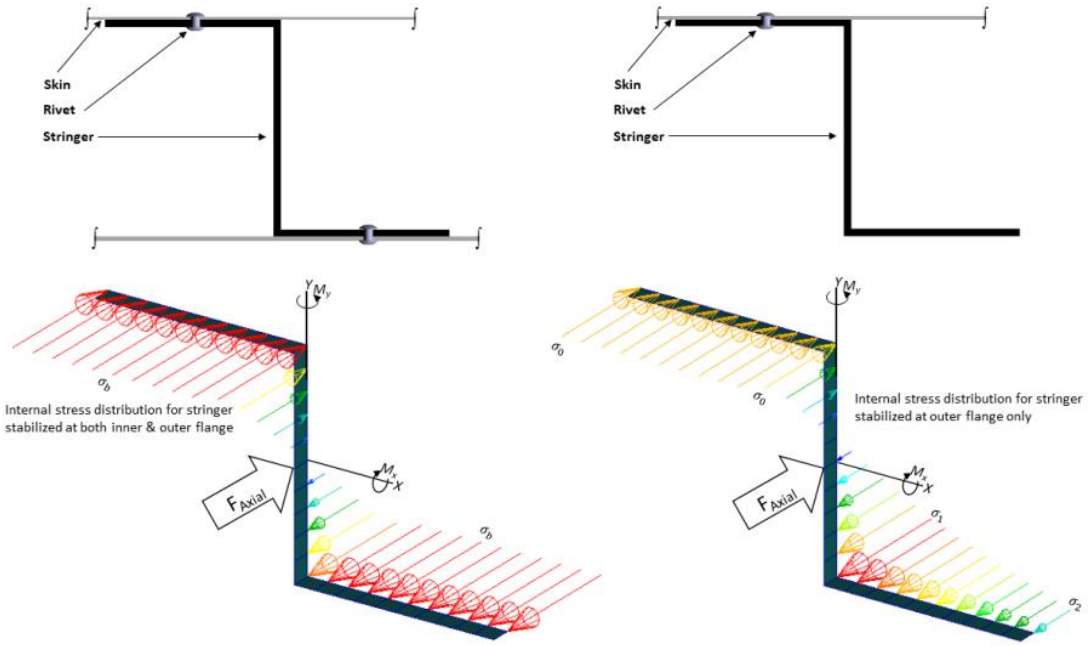

Figure 5. Comparison of stress distribution due to applied bending moment for fully and semi-stabilized stringers

This investigation examines stringer reinforcement as an example where such non-conservatism can significantly impact both the static strength and fatigue life of primary structure. The research presents a straightforward methodology for reinforcing existing unsymmetrical, semi-stabilized structures to optimize their structural performance. Finite Element Analysis (FEA) validates the proposed method's assumptions and reveals flange efficiency phenomena in semi-stabilized sections—a characteristic typically associated only with curved beam structures. The study further proposes a hypothesis explaining this phenomenon and develops a semi-empirical equation to predict the flange efficiency factor for unsymmetrical, semi-stabilized structures under bending.

3. Structural Integrity of Composite Structures

3.1 Numerical prediction of stringer de-bonding in composite stiffened panels subjected to combined axial and pull loading (D. Bardenstein, IAI)

The aerospace industry increasingly relies on bonded composite structures for their lightweight, high-stiffness properties and smooth load distribution. Despite these advantages, the adoption of bonded joints is limited due to challenges in predicting damage progression and the inadequacies of non-destructive inspection techniques. This study focuses on advancing damage-tolerant design methodologies for bonded composite structures used in aerospace applications. Conducted collaboratively by the Israel Aerospace Industries (IAI) and the U.S. Air Force Research Laboratory (AFRL), the research developed and validated a novel fail-safe concept known as the Mushroom Damage Arresting Feature (MDAF). This innovation aims to ensure controlled crack growth in adhesive bonds, prevent rapid and catastrophic failure, and improving the reliability of composite aircraft structures.

The MDAF design (presented in the figure below) introduces geometrical modifications—mushroom shapes and recesses—along the flanges of stiffened panels. These features, manufactured using water-jet techniques, create barriers that hinder the progression of debonds. Testing shows that initial damage halts at these features, requiring significantly higher loads to propagate further.

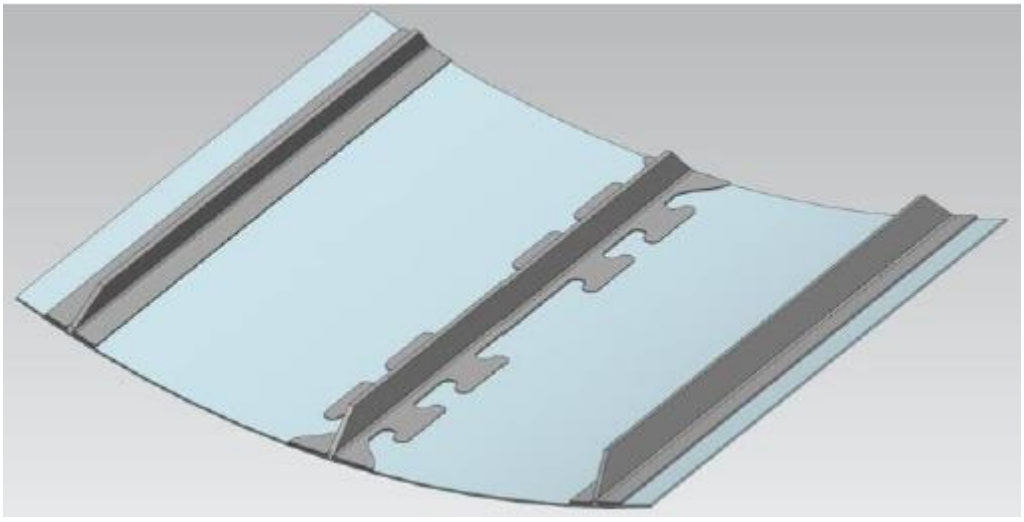

Figure 6. Test panel that is designed with the Mushroom Damage Arresting Feature (MDAF)

The study employed a combination of finite element (FE) analysis and experimental validation to assess the MDAF concept. Static and nonlinear analyses using MSC NASTRAN and PATRAN were employed to simulate damage initiation and progression. Cohesive zone modeling (CZM) was utilized to characterize adhesive properties and predict debond behavior under varying loads.

The experimental validation included Double Cantilever Beam (DCB) tests to evaluate cohesive properties of the adhesive interfaces. Single Cantilever Beam (SCB) and shear tests were performed and compared the MDAF design against reference configurations under fatigue and static loading. Stiffened panel tests examined the combined axial and pull loading behavior.

Experimental results revealed significant advantages of the MDAF concept over traditional designs. The MDAF design delayed crack propagation, with damage arrest observed at the mushroom features. Approximately 5% increase in critical load capacity was recorded for MDAF panels compared to reference panels. The damage propagation was more controlled, reflecting higher toughness rates. Numerical analyses corroborated these findings, with FEA models closely matching experimental data in most scenarios. Discrepancies were attributed to mixed interlaminar and adhesive damage modes not fully captured in the numerical simulations.

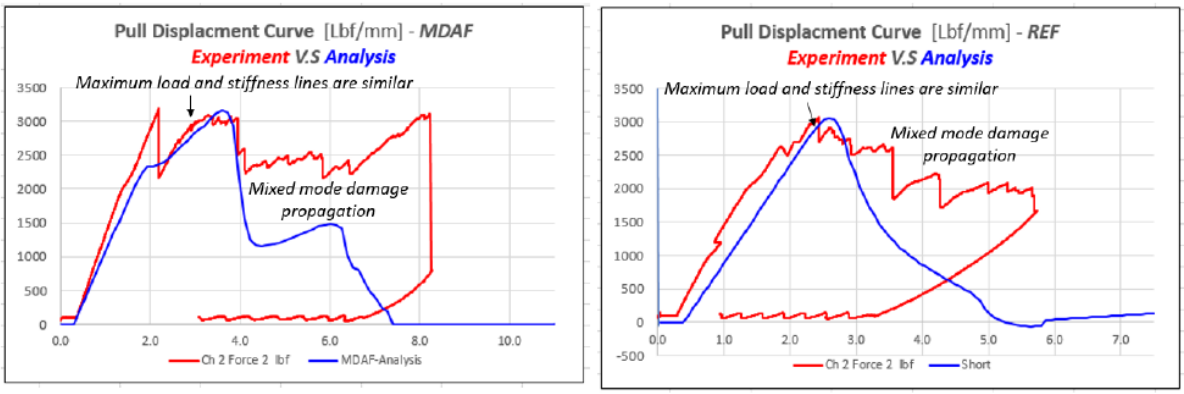

Figure 7. Comparisons of test vs. analysis load-displacement curves for MDAF and reference panels

Digital Image Correlation (DIC) strain measurements provided spatial insights into damage progression, confirming the effectiveness of the MDAF design. Strain data aligned well with numerical predictions, demonstrating the robustness of the combined experimental and computational approach.

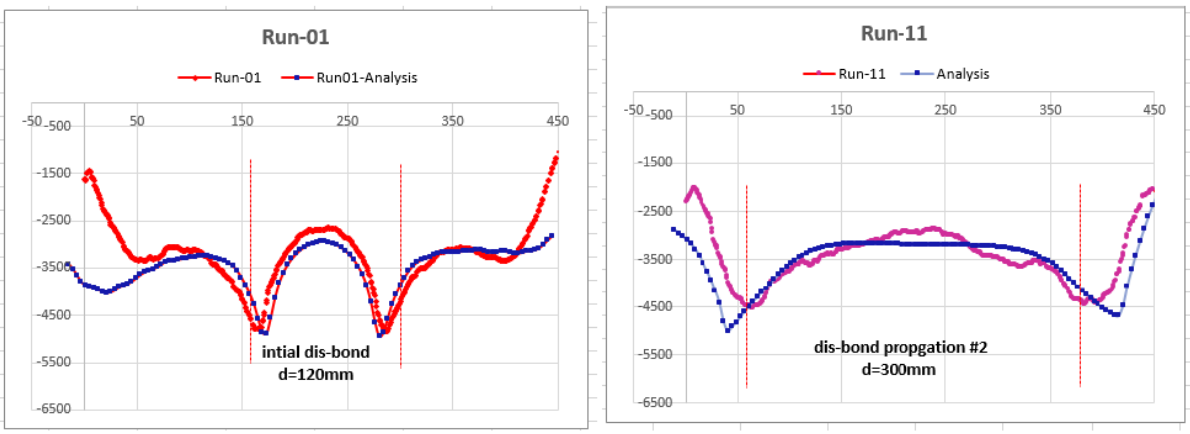

Figure 8. Comparisons of test vs. analysis strains along the mushroom

The next stage of this project included a fatigue test performed on a representative MDAF demonstrator. The figure below presents the damage evolution in the bond-line as a function of the cycles accumulated. The MDAF indeed present a slow and stable damage growth, thus allowing establishment of inspection schedule to detect such damages before reaching critical size.

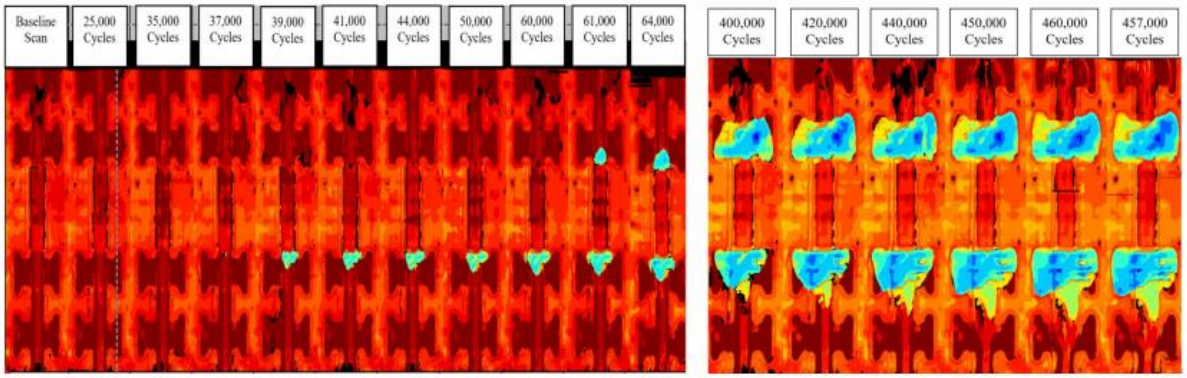

Figure 9. Damage growth at the bond line upon repeated cycling test

To conclude, this study successfully demonstrated the MDAF concept as a viable fail-safe mechanism for bonded composite structures. By arresting crack growth at predetermined locations, the design enhances structural reliability and compliance with aerospace safety standards. While the research focused on axial and pull loading conditions, further work is recommended to optimize the design for combined loading scenarios (Mode I and Mode II) and explore broader applications in other structural components like wing spars and ribs.

This work represents a significant step toward addressing the limitations of bonded composite joints, paving the way for more widespread adoption of lightweight and cost-effective bonded structures in the aerospace industry.

3.2 OPTICOMS Project – Optimized composite structures for small aircraft (Y. Freed, IAI)

The OPTICOMS project, part of the EU's Horizon 2020 program, addresses the challenges of automating composite manufacturing for the Small Air Transport (SAT) sector. Traditionally, automation has been accessible primarily to large-scale aircraft manufacturers due to high costs. OPTICOMS aims to reduce composite design and production expenses by up to 40%, decrease structural weight by 20%, and lower lifecycle costs by 20%. These improvements make advanced manufacturing techniques viable for smaller aircraft manufacturers.

Launched in 2016, the project focuses on building an integral seven-meter composite wing using innovative methods from industry leaders Coriolis, Techni-Modul Engineering (TME), and Danobat. Techniques like Automatic Fiber Placement (AFP), robotic pick-and-place systems, and Automatic Dry Material Placement (ADMP) enable high-quality, cost-effective production. The project also eliminates reliance on traditional autoclave curing, which is expensive and energy-intensive, by adopting out-of-autoclave processes.

The wing's design incorporates advanced tooling and embedded Structural Health Monitoring (SHM). SHM systems use optical fibers to monitor stress and strain, ensuring durability and aiding maintenance by predicting wear. Complementary initiatives, including FITCoW and ELADINE, contribute to the development of precision tooling to manage deformation during production. These efforts address the challenges of maintaining consistency in large composite parts, such as preventing "spring-in" distortions.

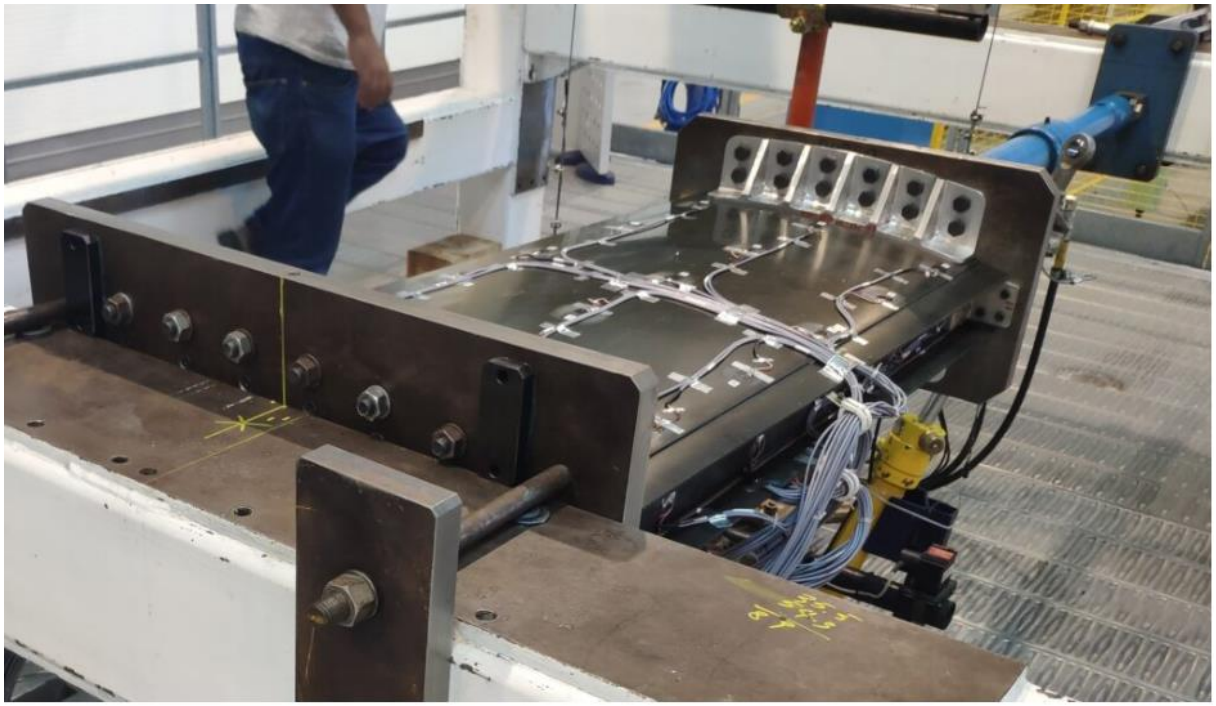

Figure 10. Assembled small scale demo test in Piaggio including optical fibers

OPTICOMS emphasizes collaboration, uniting organizations like Piaggio Aerospace, the National Institute for Aerospace Research, and the Italian Aerospace Research Centre. The project demonstrates how competitors can become collaborators, exchanging expertise to refine technologies and achieve shared goals. Preliminary results include the successful testing of small-scale demonstrators and improvements in grippers, molds, and robotic systems. These advancements pave the way for full-scale static and fatigue testing of the composite wing.

By addressing cost, weight, and production barriers, OPTICOMS aims to transform the SAT industry, creating a more accessible pathway to automation and enhancing European industrial competitiveness.

Figure 11. Multi-spar wing demonstrator at the assembly jig before skin attachment

3.3 Effect of fiber bridging on Mode I fatigue delamination behavior of uni-directional composites (L. Banks-Sills, TAU)

This two-part study [7, 8] investigates the impact of fiber bridging on mode I fatigue delamination propagation in unidirectional (UD) carbon fiber-reinforced polymer (CFRP) laminates. The research integrates experimental testing and numerical modeling to address the inaccuracies introduced by fiber bridging in energy release rate measurements and delamination growth predictions. This work advances methodologies for characterizing and designing composite materials under fatigue conditions, which are essential for aerospace applications.

The first part of the study focuses on the experimental analysis of fatigue delamination in CFRP laminates using double cantilever beam (DCB) specimens made of AS4/8552 prepreg material. Fiber bridging was identified as a key phenomenon influencing test results, causing the apparent fatigue delamination growth rate to appear slower than in real applications. This discrepancy stems from the additional resistance provided by bridging fibers, which leads to overestimated energy release rates during delamination.

Since no standardized fatigue delamination testing protocols exist for composites, the study adapted quasi-static standards (ASTM and ISO) and developed custom approaches. The Fiber bridging zone (FBZ), where fibers provide additional resistance to delamination, was measured and characterized during testing.

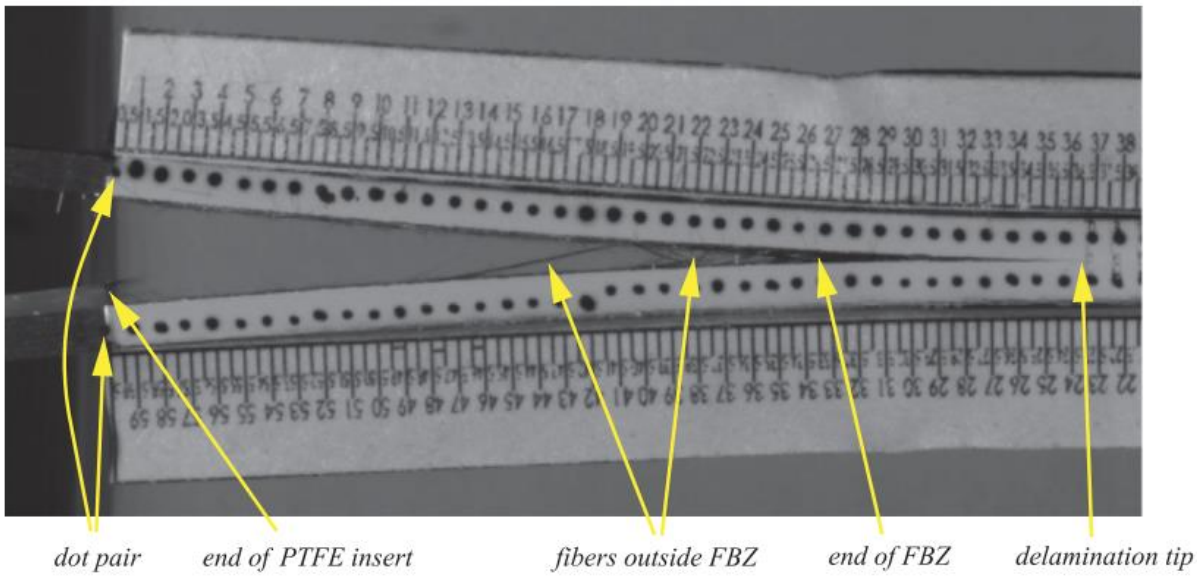

Figure 12. Fiber Bridging Zone (FBZ) in the vicinity of the delamination tip

A Paris-type relation was employed to describe the delamination growth rate as a function of the mode I energy release rate. This approach simplifies fatigue analysis by focusing on energy-based metrics rather than stress intensity factors.

The tests confirmed that fiber bridging increases the energy release rate and significantly slows apparent delamination growth, leading to overly conservative design predictions. The delamination length and FBZ dimensions were tracked using image analysis, providing data to refine predictive models. The experiments established a conservative upper bound for delamination growth, which is useful for safe composite design.

Building on these experimental findings, the second part of the study develops a cohesive zone model (CZM) to accurately simulate fatigue delamination propagation while accounting for and removing the effects of fiber bridging. The model uses a traction–separation relation (TSR) to describe the quasi-static and fatigue damage behavior of the composite material. The CZM was implemented as a user-defined element (UEL) in the finite element software Abaqus. The TSR defines the material's behavior under fatigue, including elastic deformation, damage initiation, and subsequent softening up to failure. Fatigue damage is incrementally applied at each load cycle, allowing the model to simulate the progressive degradation of the material. The model distinguishes between fiber bridging contributions and other dissipative mechanisms, such as matrix cracking and fiber–matrix separation.

Fiber bridging was shown to contribute approximately 95% of the dissipative energy release during fatigue, significantly overshadowing other mechanisms. By removing the fiber bridging effects, the CZM provided a realistic representation of delamination growth rates, avoiding the overly conservative estimates from experiments alone. The model successfully reproduced experimental data, demonstrating its effectiveness in capturing the key behaviors of fatigue delamination propagation.

Numerical simulations showed that fiber bridging increased the effective fatigue fracture toughness of the material by about 22%. This insight is critical for improving design practices, as it underscores the importance of accounting for fiber bridging to avoid over-design and material waste.

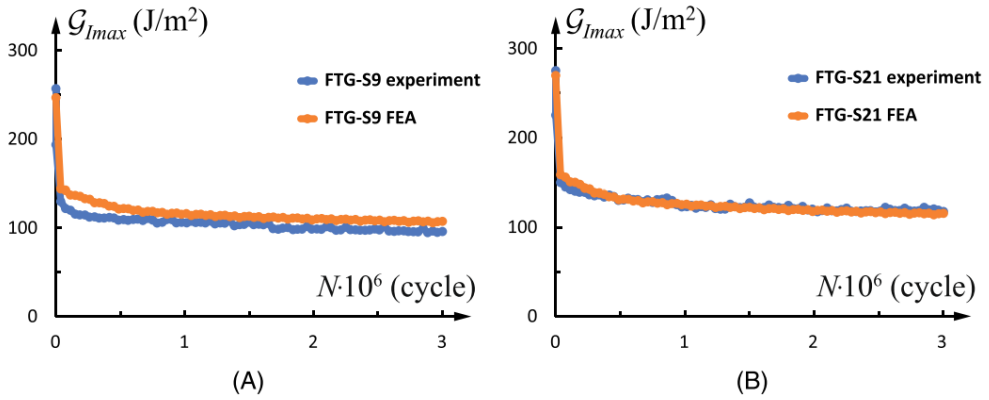

Figure 13. Experimental (blue) and finite element predictions (orange) of energy release rate versus number of cycles for two different specimens tested

This comprehensive study addresses a significant challenge in composite material testing and analysis by rigorously examining the role of fiber bridging in fatigue delamination. The experimental work in Part I provided critical data on the behavior of CFRP laminates, while the cohesive zone modeling in Part II offered a robust tool for refining delamination predictions. By combining experimental and numerical approaches, the research developed methods to isolate and eliminate fiber bridging effects, ensuring more accurate fatigue life predictions and established a framework for evaluating the true delamination behavior of composites, aiding in the development of safer and more efficient designs.

Enhanced understanding of the interplay between fiber bridging and other damage mechanisms in fatigue, contributing to the broader field of composite material science. This work is particularly relevant for the aerospace industry, where composite materials are increasingly used for their high strength-to-weight ratio. The findings support the development of more reliable tools for designing lightweight, durable structures while ensuring safety under fatigue loading.

3.4 Fracture toughness resistance curves for a delamination in CFRP MD laminate composites under mixed-mode deformation (L. Banks-Sills, TAU)

This study [18] investigates the fracture toughness resistance of delaminations in multi-directional (MD) carbon fiber-reinforced polymer (CFRP) laminate composites under mixed-mode I/II deformations. Building upon earlier results from nearly mode II tests [19], it focuses on Mixed-Mode End-Loaded Split (MMELS) specimens to understand delamination behavior in two distinct material systems: "wet-layup" and "prepreg." These systems, which differ in

manufacturing processes and structural configurations, offer valuable insights into the mechanics of delamination in diverse composite materials.

The research aims to characterize delamination resistance through fracture toughness resistance curves, known as R-curves, which describe the relationship between energy release rates and delamination extension. These curves are essential for understanding a material's ability to resist crack initiation and propagation under mixed-mode loading. Both global and local analytical approaches are employed: global analyses use experimental compliance methods, while local analyses involve three-dimensional finite element analyses (FEA) combined with displacement extrapolation and the M-integral technique. The MMELS test setup provides a straightforward means to study delamination with a nearly fixed mixed-mode ratio, making it particularly suited for this investigation.

The findings reveal distinct behaviors between the two material systems. The wet-layup system, with its woven and unidirectional (UD) plies, exhibits higher residual stresses caused by mismatched thermal expansion during curing. These residual stresses contribute additional energy during delamination propagation, influencing fracture behavior. In contrast, the prepreg system, characterized by uniform ply stacking and minimal thermal residual stresses, shows more predictable delamination behavior. Despite these differences, both systems display comparable critical energy release rates for delamination initiation (Gic) and steady-state propagation (Giss), highlighting the consistent performance of MD laminates across different configurations.

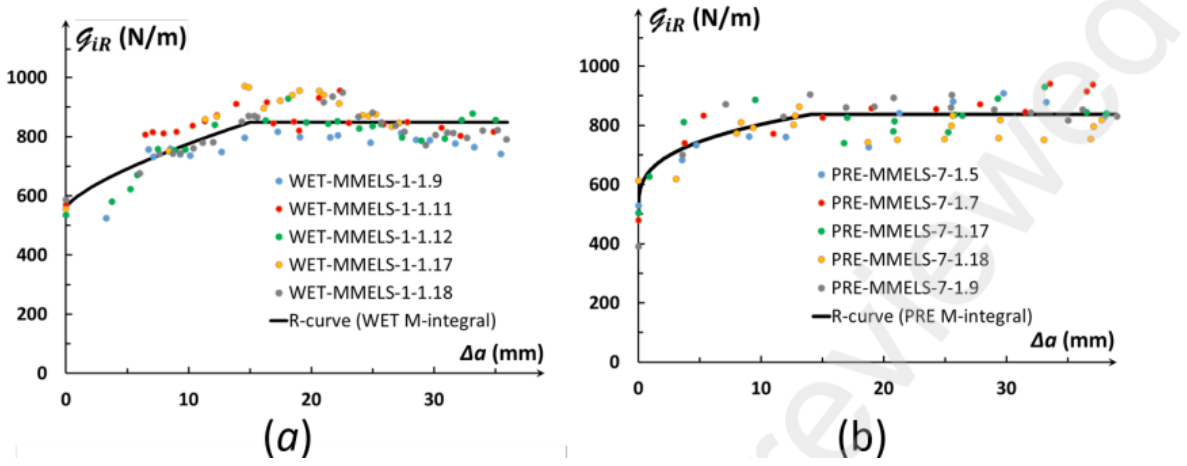

Figure 14. Resistance curves of (a) wet layups and (b) prepregs

The study also examines mode mixity by calculating stress intensity factors and phase angles. For both systems, the in-plane phase angle indicates a dominance of opening mode (mode I) deformation during delamination propagation, while the out-of-plane phase angle reveals the complex stress interactions typical of MD laminates. R-curves generated for both material systems show an increase in fracture resistance with delamination propagation. The differences between global and local analytical methods used to determine these curves are minimal—less

than 8% for the prepreg system and 12% for the wet-layup system—demonstrating the reliability of these approaches.

Thermal analyses further highlight the influence of residual stresses in the wet-layup system, where significant differences in thermal expansion between plies affect delamination behavior near specimen edges. For the prepreg system, where thermal residual stresses are minimal, only mechanical FEAs are necessary, simplifying the analysis process. These findings emphasize the role of manufacturing processes in influencing the fracture mechanics of MD laminates.

This work contributes valuable insights for industries relying on composite materials, such as aerospace, where MD laminates are prized for their high strength-to-weight ratios and resistance to environmental degradation. Understanding fracture toughness under mixed-mode loading enhances the ability to design more resilient composite structures. The comparable critical energy release rates across the two material systems suggest that MD laminates can reliably handle delaminations under mixed-mode loading, regardless of manufacturing differences. By combining global and local analytical methods, the study offers a comprehensive view of delamination mechanics, validating the methodologies for characterizing fracture toughness in complex composite systems. The results also open avenues for further research into mixed-mode behavior in other composite systems, including those with alternative layups or reinforcements, ultimately contributing to the development of stronger and more durable composite materials.

3.5 Effect of number of fatigue cycles on fatigue data for prepreg and wet layup CFRPs (L. Banks-Sills, TAU)

The study [27] explores the effect of the number of fatigue cycles on the delamination growth behavior of carbon fiber reinforced polymer (CFRP) composites, specifically those manufactured using prepreg and wet-layup techniques. Fatigue tests were conducted to understand how accurately the delamination propagation rate can be modeled using different cycle ranges. This work is critical in applications where CFRP materials are subjected to repeated loading, such as in aerospace and automotive industries, to ensure reliability and structural integrity.

The experiments employed double cantilever beam (DCB) specimens made from two distinct material systems. One consisted of a multidirectional woven prepreg laminate, while the other was a wet-layup composite. Both systems were subjected to fatigue loading under displacement control, with tests aiming to achieve three million cycles. Measurements of delamination length were obtained through imaging techniques and analyzed in relation to specimen compliance and the maximum energy release rate in each cycle. The analysis considered subsets of the total cycles, including the first 0.5, 1.0, 1.5 and the full 3.0 million cycles.

To model delamination growth, the Paris relation was employed, linking the delamination propagation rate to the energy release rate through key parameters, determined for each cycle range to evaluate the effects of shorter tests (in terms of fatigue cycles) on the accuracy of the

results. The study revealed that while shorter tests can be less time-consuming, they often yield inconsistent or unreliable estimates for the Paris governing parameters. In particular, tests using fewer cycles resulted in significant variability in these parameters, whereas tests conducted closer to the full 3.0 million cycles were much more consistent.

The findings highlighted a notable difference between the two material systems. Wet-layup specimens demonstrated greater reproducibility and accuracy compared to the prepreg specimens, a result attributed to more frequent sampling of delamination length data in the former. The study underscores the importance of longer fatigue tests to capture the complete delamination behavior and provide reliable data for modeling. For practical applications, the authors recommend conducting tests for at least 1.5 million cycles, with 3.0 million cycles being the ideal threshold.

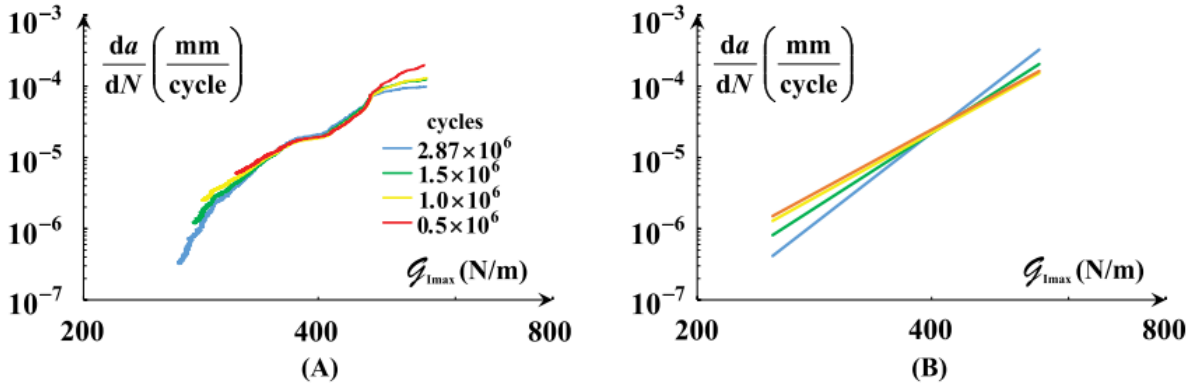

Figure 15. Delamination propagation rate vs. maximum mode I energy release rate for a specific specimen, with (a) different N_{max} and (b) curves using Paris equation with governing parameters obtained from the different tests

In conclusion, the research emphasizes that while shorter tests may seem advantageous in terms of time and resource efficiency, they risk inaccuracies in critical parameters needed for delamination growth modeling. The authors advocate for more comprehensive testing to ensure the reliability of CFRP components, particularly in safety-critical industries. This study sets the stage for further investigations into other modes of deformation and different composite material systems, ensuring broader applicability of the findings.

3.6 Fatigue delamination propagation: various effects on results (M. Mega, AU)

This investigation was performed in collaboration with the Drezer Fracture and Fatigue Laboratory at Tel Aviv University and published in Ref. 20. In this investigation, three subjects are considered. Firstly, the effect of the human factor on measurements in fatigue delamination propagation tests is examined. Delamination length measurements by different investigators reveal a limited influence of the human factor. Secondly, the influence of the R-ratio on fatigue delamination growth rates is discussed. It is observed that lower R-ratios are associated with higher propagation rates, contradicting conventional wisdom. Finally, comparisons between

fatigue propagation rates of two material systems demonstrate that energy release rates used for assessment should not be normalized.

Human Factor in Measurement:

The delamination length a is often derived as a function of specimen compliance C and the cycle number N. Many investigators capture a series of images to measure a, introducing variability due to human factors. This variability arises from subjective judgment in measuring crack lengths or interpreting images. Despite this, measurements by multiple investigators show a maximum variation of 10% in the calculated propagation rates. In the figure below, a table presents the different investigators, image sets, and the number of images used by each investigator for seven measurement sets. Below the table, the compliance is plotted against the resulting delamination length cubed, a^3.

Measurement set	M-1	M-2	M-3	M-4	M-5	M-6	M-7
Investigator	1	2	3	3	4	3	5
Image set	1	1	1	2	2	3	3
No. of images	27	27	27	32	32	30	30

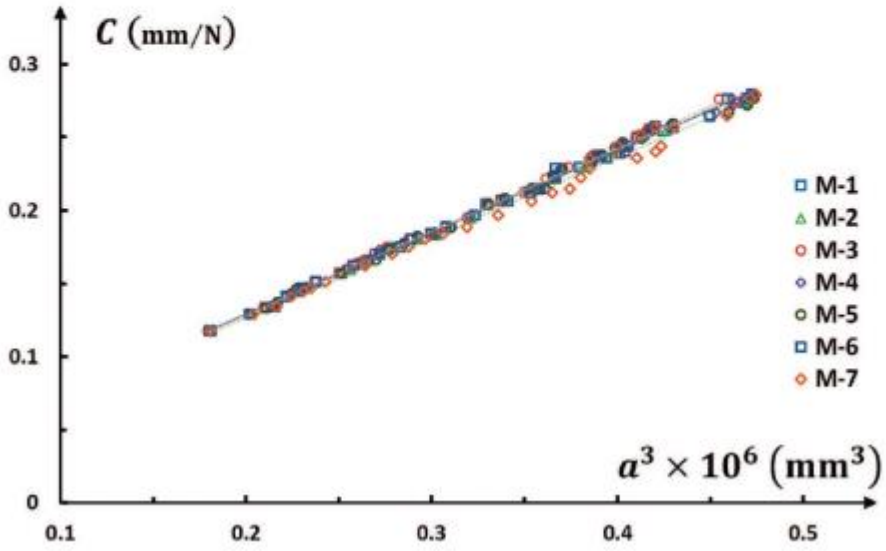

Figure 16. Comparison of compliance C vs. delamination length cubed a^3 analyzed by five investigators across seven measurement sets

The results reveal minimal variations in the delamination length measurements among the investigators, highlighting the range of variability. Future developments in automated image processing and machine learning could reduce these errors significantly. Automated systems can provide consistent measurements by analyzing delamination features pixel by pixel, thus eliminating human bias.

Influence of the R-Ratio:

The R-ratio, defined as the ratio of minimum to maximum load, is expressed as: $R_P = P_{min}/P_{max}$, where P_{min} and P_{max} are the minimum and maximum loads, respectively. The R-ratio is a critical parameter in fatigue delamination propagation. Experimental results show that delaminations propagate faster under lower R-ratios. This behavior, observed in both metals and composite laminates, emphasizes the importance of considering the R-ratio in experimental designs and data analysis. The figure below illustrates the delamination length increment, $\Delta a = a\text{-}a_0$, as a function of the number of cycles N for both prepreg and wet-layup specimens across various cyclic displacement ratios [21, 22]. For prepreg specimens, the delamination growth rate increases as the R_d-ratio decreases. A similar trend is evident for wet-layup specimens.

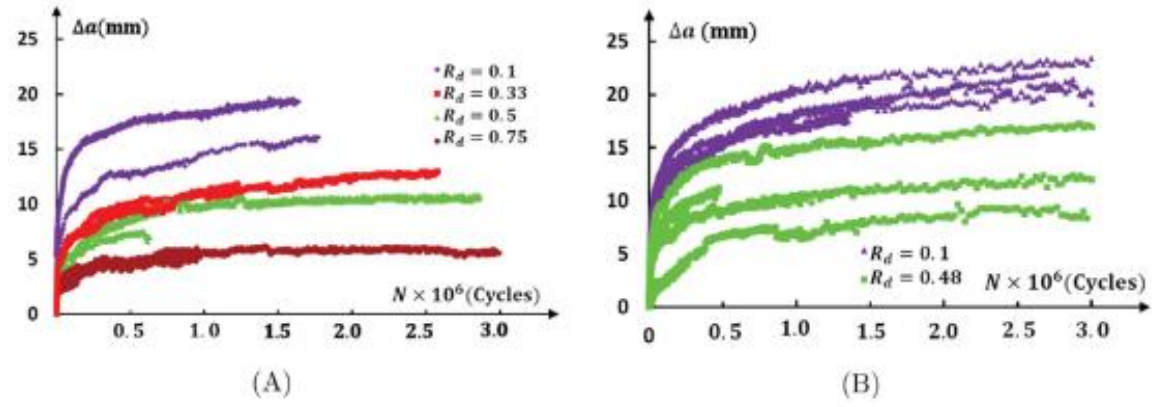

Figure 17. Delamination length increment vs. number of cycles for (a) prepreg specimens and (b) wet layup specimens

Normalization of the energy release rate:

This section compares the delamination growth rate (da/dN) of two material systems (prepreg and wet layup) as a function of both normalized and non-normalized energy release rates. Using a modified Hartman-Schijve approach for fatigue analysis, differences in fracture resistance (G_{IR}) and steady-state energy release rates (G_{Iss}) were highlighted. The fracture resistance values G_{IR} for two material systems were defined and threshold values (G_{Ithr}) were normalized.

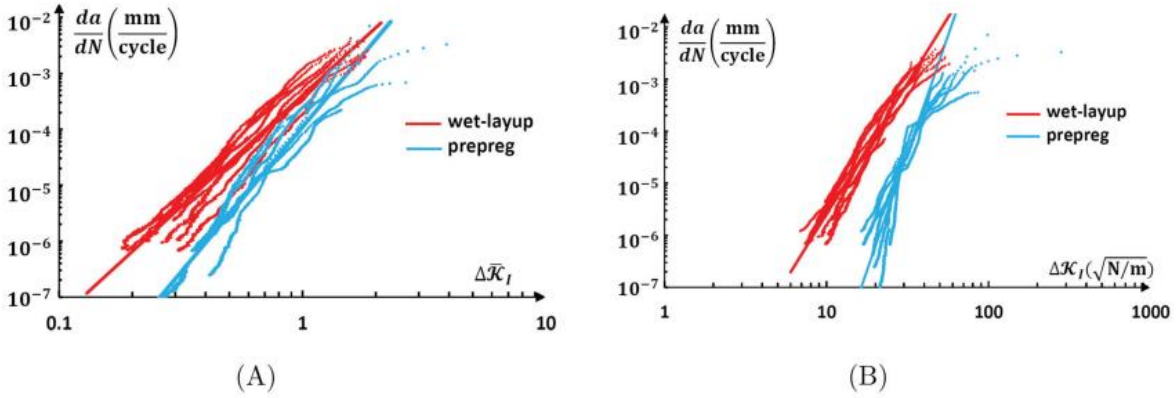

Figure 18. Delamination growth rate da/dN vs. (a) a function of the normalized maximum energy release rate and (b) the maximum energy release rate without normalization

4. Structural Health Monitoring

4.1 Real-time health monitoring of aeronautical structures via sensitivity tests utilizing principal component analysis (Y. Ofir, IAI, M. Tur, TAU)

Modern airborne structures, subjected to high maneuverability and exposed to demanding launch and landing conditions, necessitate continuous monitoring of their structural integrity and airworthiness. Structural Health Monitoring (SHM) proves particularly valuable in the case of composite aerostructures, where traditional inspection methods for critical components face challenges due to limited accessibility. An effective online SHM system can be achieved by employing fiber optic sensors, specifically Fiber Bragg Gratings (FBGs). These sensors facilitate the integration of a 'fiber optic nervous system' into the composite structure, enabling the detection, measurement, and communication of various environmental and structural parameters.

The success of an SHM system for aircraft structures relies not only on selecting the right sensors and making precise measurements but also on the processing of sensor data to derive critical information regarding operational loads and potential structural damage. Such a system allows for continuous monitoring of the structural health of these aerostructures, ensuring real-time (few seconds) assessment of their airworthiness and enabling prompt corrective actions if necessary, without the need for unnecessary grounding downtime. This holds significant strategic importance, enhancing fleet readiness and safety considerations.

Principal Component Analysis (PCA) is a well-established technique in multivariate analysis. It was first introduced by Pearson (1901), and developed independently by Hotelling (1933). PCA gained widespread recognition with the proliferation of high computing capabilities readily available in off-the-shelf computers. The core concept behind PCA is to reduce the dimensionality of a dataset containing numerous correlated variables, while preserving the majority of the data's variability. This reduction results in substantial computational efficiency without significant information loss

The process involves transforming the data into a new set of variables called principal components, which are uncorrelated and ordered in a way that the first few components capture most of the original data variation. Computing these principal components simplifies to solving an eigenvalue-eigenvector problem for a positive-semidefinite symmetric matrix. In the field of SHM, PCA has found extensive applications. It has been employed for various purposes, including the analysis of vibration signals to reduce dimensionality, eliminating environmental effects from vibration characteristics, extracting features related to structural damage, distinguishing features between damaged and undamaged structures, and classifying acoustic emission transients.

In this study [6], we utilized two PCA-based tools, the Hotelling's T-squared distribution (T^2) and the Qstatistic, as indicators of faults. These statistics have been demonstrated to exhibit high sensitivity to structural anomalies, even at small scales. When integrated into a specially designed framework, the PCA model and these statistics form a decision support tool that offers

dependable real-time information regarding the airborne structure. Such information can prove invaluable for maintenance, assessing the structure's lifespan, and making operational decisions related to mission continuity.

The performance of the method on real flight structural data (strains) was successfully demonstrated. In this case, the PCA model is based on regular flight envelope that includes standard maneuvers. The system successfully identifies a harsh maneuver that deviates from the pre-defined confidence limits, as presented below.

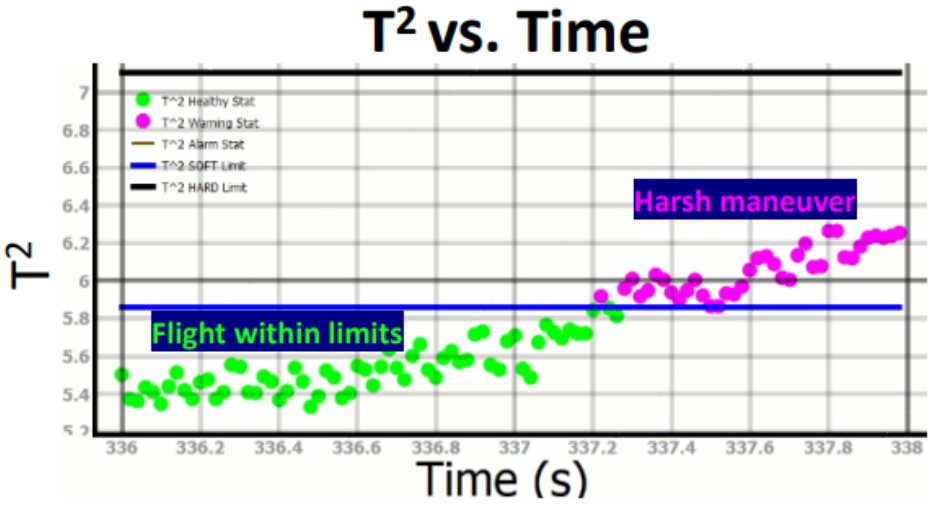

Figure 19. Deviation from flight envelope indicated by the T^2 statistic measure

4.2 Real-time structural health monitoring of composite wing in a wind tunnel test using PCA-based statistics (Y. Ofir, IAI, M. Tur, TAU)

The study focuses on employing real-time structural health monitoring (SHM) techniques to evaluate a composite wing's structural integrity during wind tunnel testing. This approach integrates advanced fiber-optic sensors with Principal Component Analysis (PCA)-based algorithms to detect damage and assess overload conditions, enabling effective and autonomous monitoring of composite structures.

A dedicated experiment utilized a specially designed composite wing embedded with a fiber-optic sensing network. This wing featured a controlled damage mechanism achieved by loosening bolts within a predefined area, enabling researchers to simulate varying levels of debonding. Fiber Bragg Gratings (FBGs) were strategically positioned along the wing's surface to capture strain data during the wind tunnel tests. These sensors provided high-resolution measurements critical for the analysis.

During testing, the wing was subjected to wind speeds ranging from 0 to 40 m/s. The healthy state of the wing was first characterized under nominal conditions to build a baseline PCA model. The PCA algorithm was applied to reduce the complexity of the data while retaining its

most critical features. The resulting model represented the healthy behavior of the structure, capturing the primary variance in the data with a single principal component accounting for nearly all data variation.

Figure 20. Composite wing located in the wind tunnel and subjected to variable wind speeds and bolt configuration settings

The PCA-based statistical measures, including Hotelling's T^2 and Q-statistics, were employed to detect deviations from the healthy model. The T^2-statistic, sensitive to changes in the primary data subspace, effectively identified overload conditions, while the Q-statistic, responsive to residuals outside the model, pinpointed damage. When the wing experienced increasing wind speeds and damage was introduced by loosening bolts, both statistical indicators showed significant deviations. The T^2-statistic highlighted overload conditions at wind speeds of approximately 35 m/s and above, marking a transition between normal and abnormal states. The Q-statistic identified damage at lower speeds, with marked deviations evident as wind speeds approached 30 m/s.

The methodology demonstrated the robustness of PCA in monitoring structural health, with the model effectively distinguishing between healthy, warning, and damaged states in real time. The placement of FBGs near areas prone to damage, coupled with the algorithm's sensitivity, enhanced the system's ability to detect anomalies. However, the study also noted that optimizing sensor placement and refining model thresholds could further improve detection accuracy. The influence of environmental factors, such as temperature fluctuations within the wind tunnel, was also considered to ensure reliable readings.

In conclusion, this research highlights the potential of fiber-optic-based SHM systems, combined with PCA, to provide dependable, real-time assessments of composite structures. By leveraging high-resolution sensors and advanced statistical algorithms, the system offers a promising solution for monitoring structural integrity in aerospace applications. Future work

could explore alternative machine learning techniques to complement or enhance the PCA-based approach, further advancing the capabilities of SHM systems.

5. Data-Science Research

5.1 Data-driven predictions of crack growth rates in aluminum 7075-T6 (Y. Freed, IAI)

Fatigue in metallic structures has been a critical issue in aviation since the mid-20th century. As metal became the dominant material for aircraft construction, fatigue cracks began to appear, leading to catastrophic failures such as the Comet I crash in 1954, the F-111 wing failure in 1969, and the Boeing 707 crash in 1977. These incidents pushed the aviation industry to develop methods for fatigue assessment and prevention.

In the 1970s, airframe fatigue analysis started to incorporate fracture mechanics concepts, notably crack growth predictions. It mainly relied on the Paris' law [12], in which a linear relationship (in a log-log scale) between crack growth rates and stress intensity was established. Subsequent studies revealed non-linearities, particularly for small and very long cracks. The stress ratio (R-ratio), which represents the relationship between minimum and maximum stress, was also found to significantly affect crack growth. Researchers developed models to refine Paris' law. Forman [11] included the R-ratio and critical fracture toughness (K_c) to account for large cracks. Elber [10] introduced the concept of crack closure, which improved predictions by considering crack behavior during cyclic loading. Willenborg [13] built on this with a load-interaction concept, further advancing crack growth modeling.

With more mature crack growth models in hand, both the military (in 1974) and the civil aviation (in 1978) sections adopted the damage tolerance concept, mandating the use of fracture mechanics for airframe design, leading to inspection programs aimed at detecting cracks before they reach critical sizes. The need for improved crack growth predictions in metallic structures remains a priority.

Recently, advancements in computational power have enabled data-driven approaches to simulate complex phenomena more efficiently. Neural networks and support vector regression (SVR) have been used to predict fatigue crack growth in various materials. Studies [9, 14] applied these methods to materials like aluminum and titanium, demonstrating their effectiveness in predicting crack growth. This study, presented in Ref. [15], focuses on developing a surrogate model to predict crack growth in 7075-T6 aluminum, an alloy commonly used in aviation. The crack growth behavior of this alloy is complex, influenced by factors such as stress intensity range (ΔK), R-ratio, and specimen thickness. Observed non-linearities, particularly in the range of $8 < \Delta K < 12$, add complexity to predictions, as presented in Figure 21.

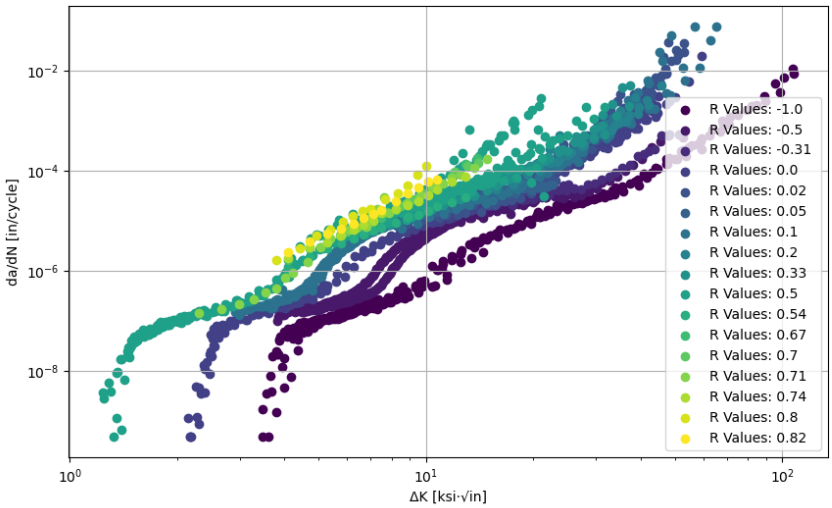

Figure 21. Crack growth behavior for 7075-T6 with different R-ratios

To address this complexity, four different machine learning regression algorithms are studied: Random Forest (RF), Gaussian Process Regression (GPR), K-Nearest Neighbors (KNN), and Kernel Regression (KR). Their performance is evaluated and the most promising algorithm is selected to predict the crack growth of aluminum 7075-T6 under various fatigue stress spectra. Figure 22 presents the performance of the different methods with respect to validation data. While all regression techniques yield reasonable regressions, they fall short in comparison to the predictive accuracy achieved by Random Forest regression.

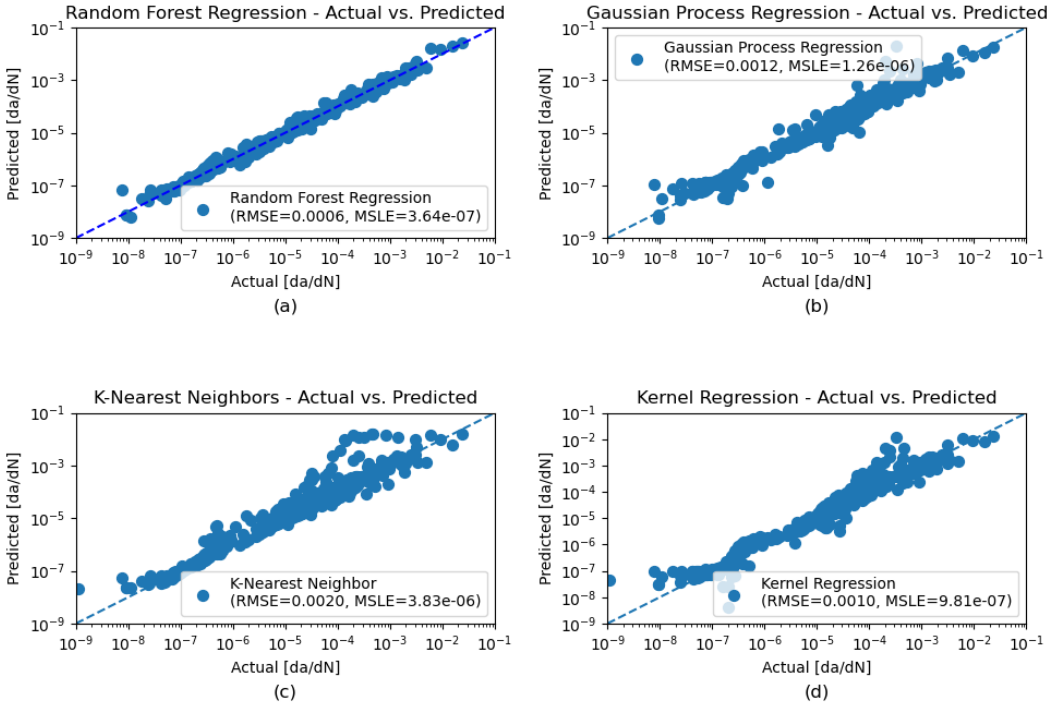

Figure 22. Predictions vs. actual algorithm test data by means of (a) Random Forest regression, (b) Gaussian Process Regression, (c) K-Nearest Neighbors regression and (d) Kernel regression

The performance of the proposed approach with respect to variable amplitude spectra is evaluated in this study. Two cases of variable amplitude spectra are studied. Load interaction correction factors are incorporated into the predictions, presented in Figure 23. As can be seen from this figure, the interaction correction factors are significant and should be employed for predictions. Overall, the Random Forest regression demonstrated excellent accuracy in predicting the experimental results.

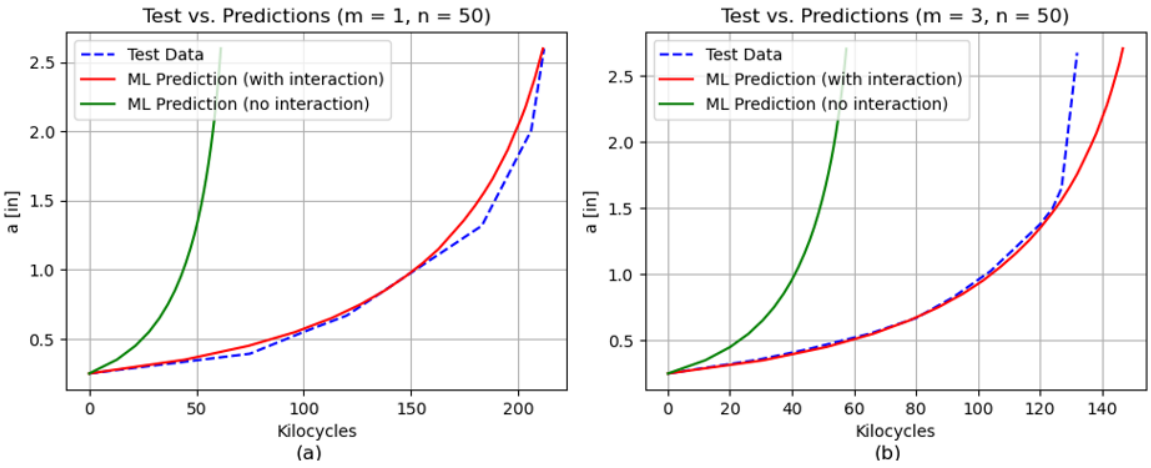

Figure 23. Validation of crack growth data regression performed using Random forest algorithm

The full-length paper [15] includes a through explanation of the methodology used in this study as well as additional discussion on the predictions and their accuracy.

5.2 Machine Learning Compliance Calibration for Fatigue Energy Release Rate in Laminates (M. Mega, AU)

This study [23] investigates the fatigue behavior and delamination resistance of multidirectional composite laminates subjected to cyclic loading. The focus is on the influence of fiber bridging during delamination propagation and the comparison of local versus global methods for calculating the energy release rate (ERR). Seven unidirectional (UD) and multidirectional (MD) composite laminate layups were analyzed, each representing a different arrangement of fiber orientations. The study employed two primary methods to calculate the ERR: the local J-integral method in conjunction with numerical finite element analyses, which focuses on the energy at the crack tip, and the global modified compliance calibration ((MCC) method, which considers the overall response of the laminate.

Key observations:

- Fatigue Resistance and Fiber Orientation: The fatigue resistance of MD composite laminates varied significantly based on fiber orientation. Layups with fiber orientations such as 90°/90°, 0°/45°, and 0°/90° demonstrated enhanced fatigue resistance, primarily

due to the presence of fiber bridging across delaminated interfaces. This bridging effect helps to resist further propagation of the delamination. In contrast, layups like 45°/45° and 0°/0° showed less fatigue resistance due to limited or no bridging mechanisms.

- Fiber Bridging Effects: Fiber bridging was observed to significantly influence the delamination toughness. It was particularly beneficial in longer delaminations, where fibers linking the two delaminated surfaces acted to resist the propagation of the crack. This resulted in improved delamination growth resistance and higher overall toughness. The fiber bridging effect was most noticeable in composite laminates with longer delaminations, where saturation of the bridging effects occurred.

- Stiffness Variation with Delamination Length: The stiffness of the composite laminate increased with delamination length, particularly due to the fiber bridging mechanism. This behavior was observed in both UD and MD composites, where the delaminated zone grew, leading to more consistent material properties. However, short delaminations exhibited more variability in mechanical properties.

- Complex Delamination Behavior and Migration: In some laminate configurations, such as the 90°/90° interface, delamination propagation showed complex behaviors, including front oscillations and splitting. These phenomena posed challenges for traditional linear elastic fracture mechanics (LEFM) analysis, especially in the early stages of delamination. These complex behaviors highlight the need for more advanced fracture mechanics approaches to predict delamination growth accurately in such cases.

- Paris Plot and Fatigue Resistance: Paris plots, shown in the figure below, which relate the delamination propagation rate (da/dN) to the energy release rate (G_{Imax}), were constructed for both UD and MD layups. These plots revealed that the delamination propagation rate decreases as the delamination length increases, which is consistent with the increased effectiveness of fiber bridging mechanisms. The Paris plots demonstrated that MD composites, particularly those with higher fiber bridging, exhibited better fatigue resistance.

- Calibration of Material Properties: A comparison of calibrated material properties with those found in the literature indicated that the calibrated properties, which include fiber bridging effects, provided a more accurate prediction of delamination behavior. The calibrated properties led to higher G_{Imax} values, improving the accuracy of simulations and offering a better representation of real-world fatigue behavior.

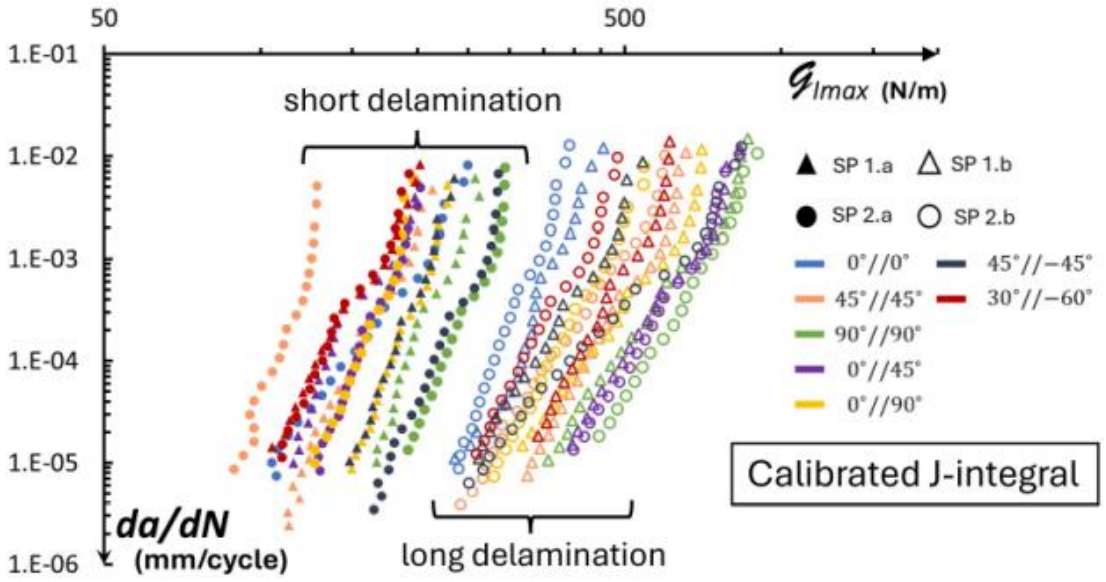

Figure 24. The delamination propagation rate da/dN plotted on a log-log scale against the maximal mode I energy release rate in a fatigue cycle, calculated with the J-integral using calibrated material properties in the simulations for seven MD composite layups

In conclusion, this study highlights the crucial role of fiber bridging in enhancing the fatigue resistance of MD composite laminates. The incorporation of fiber bridging effects into material models leads to a more accurate simulation of delamination propagation, allowing for better predictions of fatigue performance. The results also suggest that future work should focus on standardizing testing protocols for composite laminates under fatigue loading and exploring the role of fiber bridging in more complex delamination behaviors.

5.3 Transfer Learning for Fractographic Analysis in Additive Manufacturing (M. Mega, AU)

This study [24] aimed to enhance the detection and characterization of fatigue crack initiation sites in additively manufactured (AM) materials using automated machine learning techniques. The material investigated was Titanium Ti-6Al-4V, manufactured via selective laser melting (SLM), a process prone to defects that compromise fatigue performance. The investigation employed a combination of convolutional neural networks (CNNs) and object detection models to analyze fractographic images captured through scanning electron microscopy (SEM).

High-resolution SEM images from fatigue-tested specimens were divided into regions of interest (ROIs) for analysis. A ResNet152 CNN model [25] was trained to classify these ROIs, isolating areas with potential crack initiation sites with an accuracy of 97.6%. Subsequently, YOLOv5 [26], a state-of-the-art object detection algorithm, was used to detect and classify specific defect features in these regions, achieving an 82.3% detection accuracy. An example of the annotation of YOLOv5 dataset is demonstrated in the figure below.

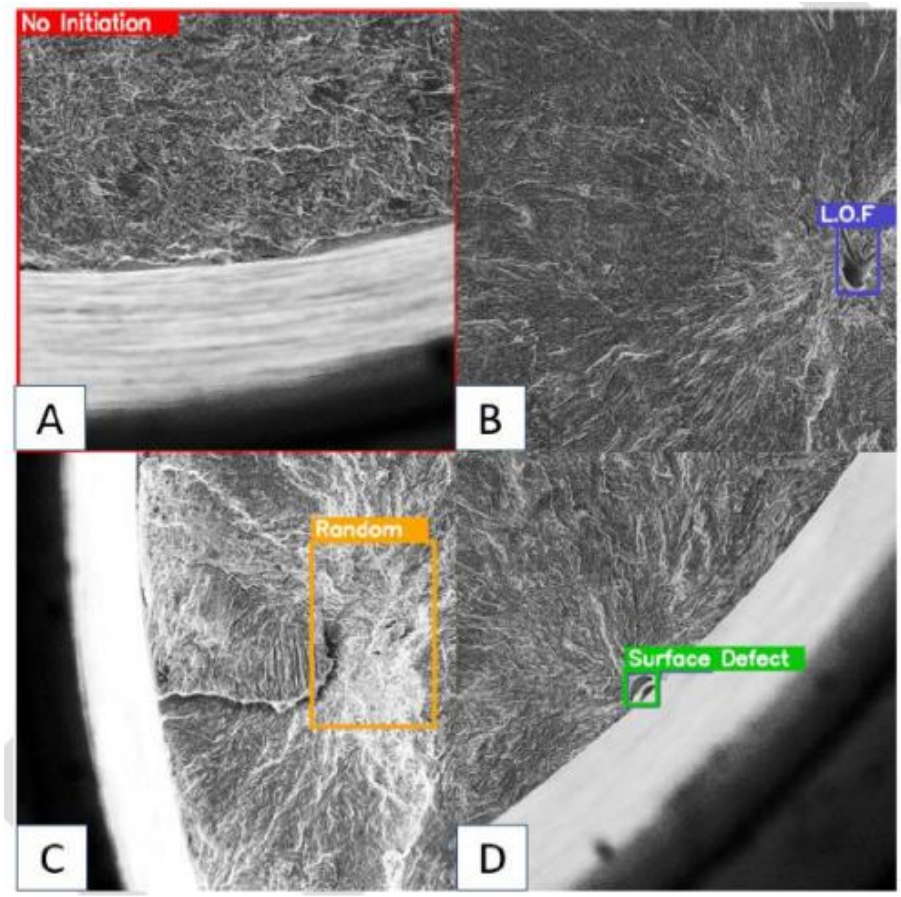

Figure 25. Example of annotation of YOLOv5 dataset. (a) an image that does not contain the initiation sire (red), (b) an image containing a Lack of Fusion (LOF) defect (purple), (c) an image containing a random initiation site (orange) and (d) an image containing a LOF defect which is also a surface defect (green)

The automated workflow significantly reduced manual analysis time and provided consistent, reproducible results. Computer vision techniques were integrated to calculate the spatial relationship between crack initiation sites and the specimen surface, a metric crucial for correlating defect location with fatigue life. The error in distance measurement was quantified at 33.7 µm, corresponding to a relative error of 19.2%.

6. Miscellaneous

6.1 Surface quality challenge for Ti-6Al-4V additive manufactured topologic optimized lightweight structure (C. Matias, IAI)

The paper [28] explores the challenges and experimental evaluation of surface quality improvement techniques for Ti-6Al-4V additive-manufactured (AM) structures optimized topologically for lightweight aerospace applications. It emphasizes the importance of surface quality in ensuring fatigue strength for airframe structural components, which are often subjected to cyclic loading. The inherent roughness and defects of AM surfaces, coupled with the geometric complexity of topologically optimized designs, present significant obstacles for traditional surface treatment methods.

The study employs a Universal Component Specimen (UCS), designed to represent complex structural features typical of topologically optimized AM parts. This specimen includes multiple load paths, hidden radii, and areas of stress concentration, simulating real-world scenarios for fatigue testing. The UCS was manufactured using selective laser melting technology, utilizing a Ti-6Al-4V alloy, and then subjected to various state-of-the-art surface improvement treatments.

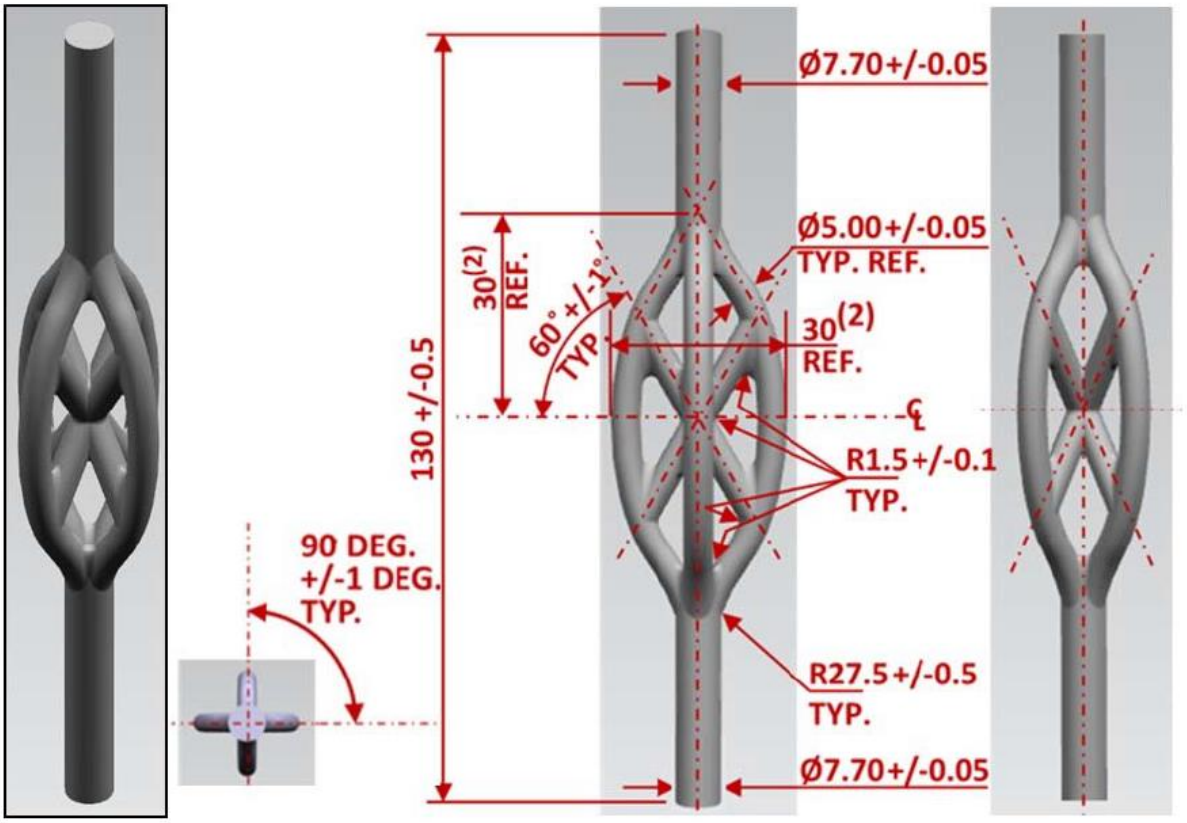

Figure 26. UCS specifications

The research examines six surface treatment techniques, including chemical and electrochemical methods, high-frequency movement in liquid media, dry electropolishing, plasma electrolytic polishing (PeP), and a combination of powder blasting with PeP. Each method was evaluated based on its impact on the fatigue life of the specimens, with the untreated "as-built" condition serving as the baseline. While some techniques demonstrated improvements in fatigue life, none achieved the necessary enhancement to meet the fatigue requirements for airframe structural applications.

The findings highlight the limitations of current surface treatment methods in addressing the localized defects and surface quality variations inherent to AM processes. The fatigue performance remained insufficient, as evidenced by Weibull statistical analyses and fractographic studies. These analyses revealed that even treated surfaces often exhibited significant defects, compromising fatigue strength. The best-performing techniques improved fatigue life by factors ranging from 1.14 to 3.03 over the baseline, far below the required factor of 17 to meet aerospace standards.

The study concludes that achieving the required surface quality for AM structural components in aerospace demands further development and innovation in surface treatment techniques. It suggests combining surface improvement methods with surface enhancement technologies, such as laser shock peening or photo-peening, to achieve better results. Additionally, it advocates for the integration of surface quality considerations during the early design phases of AM parts to ensure compliance with fatigue and damage tolerance requirements.

Overall, this research underscores the need for continued exploration and optimization of surface treatment technologies to fully realize the potential of additive manufacturing in the aerospace industry.

6.2 From macro fracture energy to micro bond breaking mechanisms – Shorter is tougher (D. Sherman, TAU)

The publication [16] explores innovative fracture behaviors and mechanisms in brittle materials by bridging macro- and microscale analyses. Using a combination of experimental techniques and Molecular Dynamics (MD) simulations, the study provides new insights into energy dissipation and crack propagation in single-crystal silicon. The authors challenge traditional theories, particularly Griffith's theory, by identifying unique properties and mechanisms in brittle materials.

Griffith's theory postulates that the energy required to propagate a crack is determined by the balance of surface energy and elastic strain energy. However, the study reveals that the cleavage energy of brittle materials is not constant, as Griffith suggested, but instead bounded by a lower limit (the Griffith barrier) and an upper limit (the lattice-trapping barrier), which can be up to three times higher. This variability is influenced by factors such as precrack length and the gradient of the Energy Release Rate (ERR), denoted as Θ.

The authors conducted dynamic fracture experiments on single-crystal silicon, focusing on the energy-speed relationship and crack front behavior. They observed that the cleavage energy, Γ0, increases with Θ, which is influenced by the precrack length. Specimens with shorter precracks demonstrated higher cleavage energy requirements, leading to the counterintuitive conclusion that shorter cracks are tougher. This phenomenon challenges the traditional Griffith framework and suggests that cleavage energy is not solely a function of material properties but also depends on the geometry and loading conditions.

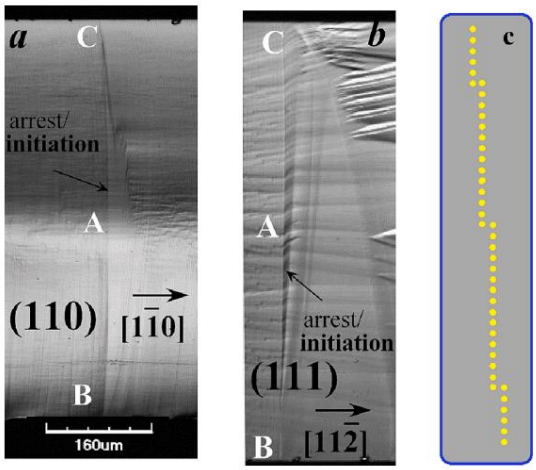

Figure 27. Optical microscope images of the fracture surfaces of silicon specimens cleaved under tension during crack initiation, propagation and arrest cycles

To investigate the underlying mechanisms, the authors performed MD simulations to study bond-breaking processes along the crack front. They identified two primary mechanisms: low-energy kink advance (migration) and high-energy kink formation (nucleation). Kink advance involves the propagation of bond-breaking along an already-formed crack front, while kink formation requires additional energy to create new kinks. These mechanisms are influenced by the energy gradient, Θ, with higher Θ values leading to a greater contribution from kink formation. The study also highlighted that the crack front in silicon crystals is curved, a feature attributed to the presence of kinks along the crack path.

A significant contribution of the study is the identification of a transitional fracture mechanism termed "quasi-propagation." This mechanism bridges the initiation and propagation phases of fracture. During quasi-propagation, cracks grow slowly and stably for a short distance, allowing for an increase in cleavage energy from the Griffith barrier to the level dictated by Θ. This mechanism is absent at very low Θ but becomes prominent as Θ increases. It highlights the dynamic nature of fracture processes, particularly in brittle materials.

The findings also introduce the concept of a "pseudo R-curve" in brittle materials, analogous to the R-curve behavior seen in ductile materials. In this framework, the cleavage energy increases during crack growth due to the transition from kink advance-dominated mechanisms to kink

formation-dominated mechanisms. This behavior underscores the complexity of fracture processes and the importance of considering both macro- and microscale phenomena.

The study concludes that shorter precracks lead to higher material strength, a phenomenon summarized as "shorter is tougher." This is attributed to the increased cleavage energy required for crack propagation in shorter cracks, driven by higher Θ values. The research also introduces new material properties which relates the cleavage energy to the ERR gradient and the energy required for kink formation. These properties provide a deeper understanding of fracture processes and material behavior.

A follow-up study is presented in Ref. 17. This study investigates the upper bound of cleavage energy in single-crystal silicon, also challenging traditional assumptions of Griffith's theory, demonstrating that cleavage energy can exceed the Griffith energy barrier significantly, particularly in specimens with shorter precracks. Using the CTEM method, the authors examined silicon's two low-energy cleavage systems, (110)[110] and (111)[112]. Short precracks (2–5 mm) resulted in higher gradients of energy release rate Θ, leading to increased cleavage energy. Long precracks exhibited energy near the Griffith barrier and were dominated by low-energy kink advance mechanisms. In contrast, short precracks activated high-energy kink formation mechanisms, which dissipated more energy during a "quasi-propagation" phase of crack growth. The study found that the upper bound of cleavage energy reached up to 8.84 J/m^2, over three times the Griffith barrier under ambient conditions.

Overall, these investigations advance the understanding of brittle fracture by integrating macro- and microscale analyses. It challenges established theories, such as Griffith's, by demonstrating the variability of cleavage energy and introducing new fracture mechanisms. The insights gained from this work have implications for designing stronger materials and understanding failure mechanisms in brittle solids, particularly at the atomic scale. The findings also pave the way for further exploration of fracture behaviors in other brittle materials and their potential applications in engineering and materials science.

7. References

1. Freed Y., “Review of Aeronautical Fatigue Investigations in Israel, January 2021 – December 2022”, Minutes of the 38th ICAF Conference, 2023.

2. Petel, A., Jager, A., Babai, D., Jopp, J., Bussiba, A., Perl, M., Shneck, R.Z. Fatigue Crack Growth in a Monocrystal and Its Similarity to Short-Crack Propagation in a Polycrystal of Nickel, Metals 2023, 13, 790. (DOI: https://doi.org/10.3390/met13040790)

3. Aziz F, Kamal SM, Perl M, Chetry A. Increasing the load carrying capacity of hollow rotating disks by applying rotational autofrettage. European Journal of Mechanics-A/Solids. 2024 May 1;105:105231. (DOI: https://doi.org/10.1016/j.euromechsol.2024.105231)

4. Ma Q, Levy C, Perl M. The Change in the SIF of an Internal Semi-Elliptical Surface Crack Due to the Presence of an Adjacent Nonaligned Corner Quarter-Circle Crack in a Semi-Infinite Plate Under Remote Bending. InPressure Vessels and Piping Conference 2023 Jul 16 (Vol. 87455, p. V002T03A051). American Society of Mechanical Engineers.(DOI: https://doi.org/10.1115/PVP2023-105374)

5. Levy C, Perl M, Ma Q. Mode I and Mode II Stress Intensity Factors for a Slanted-Edge-Crack Affected by an Adjacent Horizontal Crack Under Remote Tension. In: Pressure Vessels and Piping Conference 2024 Jul 28 (Vol. 88483, p. V002T03A089). American Society of Mechanical Engineers

6. Ofir Y, Ben-Simon U, Shoham S, Kressel I, Bohbot J, Tur M, Real-Time Health Monitoring of Aeronautical Structures via Sensitivity Tests Utilizing Principal Component Analysis, 63rd Israel Annual Conference on Aerospace Sciences, IACAS 2024, Tel Aviv, Israel

7. Banks-Sills L, Gur HB. The effect of fiber bridging on mode I fatigue delamination propagation—part I: Testing. Fatigue & Fracture of Engineering Materials & Structures. 2024.

8. Ben Gur H, Banks-Sills L. The effect of fiber bridging on mode I fatigue delamination propagation—Part II: Cohesive zone model. Fatigue & Fracture of Engineering Materials & Structures. 2024 Oct;47(10):3529-45.

9. Bao, H., Wu, S., Wu, Z., Kang, G., Peng, X. and Withers, P.J., "A machine-learning fatigue life prediction approach of additively manufactured metals", Engineering Fracture Mechanics, 242, p.107508, 2021 (DOI: https://doi.org/10.1016/j.engfracmech.2020.107508)

10. Elber, W., "Fatigue crack closure under cyclic tension", Engineering Fracture Mechanics, 2, p. 37-45, 1970 (DOI: https://doi.org/10.1016/0013-7944(70)90028-7)

11. Forman, R.G., Kearney, V.E and Engle, R.M., "Numerical analysis of crack propagation in cyclic-loaded structure", Journal of Basic Engineering, 89, p. 459-464, 1967 (DOI: https://doi.org/10.1115/1.3609637)

12. Paris, P.C., Gomez, M. and Anderson, W.E., "A rational analytic theory of fatigue", Trends in Engineering, 13, University of Washington, USA, 1961

13. Willenborg, J., Engle, R.M. and Wood, H.A., "A crack growth retardation model using effective stress concept", AFFDL-TM-71-FBR, Wright Patterson Air Force Laboratory, 1971

14. Zafar, M.H., Younis, H.B., Mansoor, M., Moosavi, S.K.R., Khan, N.M. and Akhtar, N. "Training deep neural networks with novel metaheuristic algorithms for fatigue crack growth prediction in aluminum aircraft alloys", Materials, 15(18), p.6198, 2022 (DOI: https://doi.org/10.3390/ma15186198)

15. Freed Y. Machine Learning-Based predictions of crack growth rates in an aeronautical aluminum alloy. Theoretical and Applied Fracture Mechanics. 2024 Apr 1;130:104278.

16. Shaheen-Mualim M, Kovel G, Atrash F, Ben-Bashat-Bergman L, Gleizer A, Ma L, Sherman D. From macro fracture energy to micro bond breaking mechanisms–Shorter is tougher. Engineering Fracture Mechanics. 2023 Sep 1;289:109447.

17. Ma L, Sherman D. A search for the upper bound of the cleavage energy of silicon crystal. Engineering Fracture Mechanics. 2024 Mar 25;299:109966.

18. Mega M, Dolev O, Banks-Sills L. Fracture toughness resistance curves for a delamination in CFRP MD laminate composites, Part II: Mixed-mode deformation. Theoretical and Applied Fracture Mechanics. 2024 Oct 1;133:104583.

19. Mega M, Dolev O, Banks-Sills L. Fracture toughness resistance curves for a delamination in CFRP MD laminate composites, Part I: Nearly mode II deformation. Theoretical and Applied Fracture Mechanics. 2022 Jun 1;119:103335.

20. Anuwedita Singh, Snir Aizen, Mor Mega, Shira Rifkind, and Leslie Banks-Sills. Fatigue delamination propagation: Various effects on results. Fatigue and Fracture of Engineering Materials and Structures, 47(2):275–297, February 2024

21. T. Chocron and L. Banks-Sills. Nearly mode I fracture toughness and fatigue delamination propagation in a multidirectional laminate fabricated by a wetlayup. Phys. Mesomech., 22:107–140, 2019.

22. I. Simon, L. Banks-Sills, and V. Fourman. Mode I delamination propagation and R-ratio effects in woven composite DCB specimens for a multi-directional layup. Int. J. Fatigue, 96:237–251, 2017.

23. Roy Amkies, Mike van der Panne, John-Alan Pascoe, and Mor Mega. Machine learning compliance calibration for local fatigue energy release rate calculations in multi-directional laminates with fiber bridging. 2024. Submitted for publication.

24. Or Haim Anidjar, Ro'i Lang, and Mor Mega. Transfer learning methods for fractographic detection of fatigue crack initiation in additive manufacturing. IEEE Access, 12:6262–6280, 2024.

25. Kaiming He, Xiangyu Zhang, Shaoqing Ren, and Jian Sun. Deep residual learning for image recognition. In Proceedings of the IEEE conference on computer vision and pattern recognition. IEEE, 2016.

26. Zexuan Guo, Chensheng Wang, Guang Yang, Zeyuan Huang, and Guo Li. MSFT-YOLO: Improved YOLOv5 based on transformer for detecting defects of steel surface. Sensors, 22:3467, 2022.

27. Banks-Sills L, Choron T, Simon I. Effect of number of fatigue cycles on fatigue data: CFRP (prepreg and wet-layup). Fatigue & Fracture of Engineering Materials & Structures. 2024 Mar;47(3):833-48.

28. C. Matias, A. Diskin, O. Golan, G. Andrey, E. Strokin, Surface quality challenge for Ti-6Al-4V additive manufactured topologic optimized lightweight structure, 34th Congress of the International Council of the Aeronautical Sciences, Florence, Italy, 2024.